PNAS PLUS

Two miRNA clusters, *miR-34b/c* and *miR-449*, are essential for normal brain development, motile ciliogenesis, and spermatogenesis

Jingwen Wu[a,b,c], Jianqiang Bao[a,1], Minkyung Kim[d,1], Shuiqiao Yuan[a,1], Chong Tang[a,1], Huili Zheng[a], Grant S. Mastick[d], Chen Xu[b,c,2], and Wei Yan[a,2]

[a]Department of Physiology and Cell Biology, University of Nevada School of Medicine, Reno, NV 89557; [b]Department of Histology and Embryology, Shanghai Jiao Tong University School of Medicine, Shanghai 200025, China; [c]Shanghai Key Laboratory of Reproductive Medicine, Shanghai 200025, China; and [d]Department of Biology, University of Nevada, Reno, NV 89557

Edited by David P. Bartel, Massachusetts Institute of Technology, Cambridge, MA, and approved June 10, 2014 (received for review April 28, 2014)

Ablation of a single miRNA gene rarely leads to a discernable developmental phenotype in mice, in some cases because of compensatory effects by other functionally related miRNAs. Here, we report that simultaneous inactivation of two functionally related miRNA clusters (*miR-34b/c* and *miR-449*) encoding five miRNAs (miR-34b, miR-34c, miR-449a, miR-449b, and miR-449c) led to sexually dimorphic, partial perinatal lethality, growth retardation, and infertility. These developmental defects correlated with the dysregulation of ∼240 target genes, which are mainly involved in three major cellular functions, including cell-fate control, brain development and microtubule dynamics. Our data demonstrate an essential role of a miRNA family in brain development, motile ciliogenesis, and spermatogenesis.

forebrain | egg transport | airway obstruction | oviduct

MicroRNAs (miRNAs) comprise a highly conserved set of small RNA species encoded by eukaryotic genomes. miRNAs exert their function posttranscriptionally by binding the 3′ UTRs of their target mRNAs, thereby controlling mRNA stability and translational efficiency (1, 2). One miRNA can target numerous mRNAs, whereas the 3′ UTR of a particular mRNA can be bound by multiple miRNAs. Therefore, miRNAs and their target mRNAs form an interwoven regulatory network characterized by a reciprocal “one-to-multiple” relationship, which has been hypothesized as a “fail-safe” mechanism to control gene expression (1, 3).

Many miRNA genes exist in clusters and thus are cotranscribed and processed (3–5). Moreover, many miRNAs contain the same seed sequences and, by definition, belong to functionally related miRNA families (6, 7). For example, the miR-449 miRNA cluster encodes three miRNAs (miR-449a, miR-449b, and miR-449c), and the miR-34b/c cluster encodes two (miR-34b and miR-34c) (8–11). All five miRNAs have the same seed sequence, which is also shared by another miRNA, miR-34a (8, 9, 11). Therefore, these six miRNAs form a functionally related miRNA family. Single KO mice deficient of *miR-34a*, *miR-34b/c*, or *miR-449* display no discernible phenotype, however (8, 11, 12).

Given the overlapping spatiotemporal expression patterns between *miR-34b/c* and *miR-449* in the testis (8), we generated double KO (dKO) mice lacking both miRNA clusters. Here we report that the *miR-34b/c* and *miR-449* clusters are functionally redundant and, importantly, that simultaneous inactivation of these two miRNA clusters disrupts their target genes involved in cell fate control, brain development, and microtubule dynamics, leading to underdeveloped basal forebrain structures, absence of motile cilia in trachea and oviducts, and severely disrupted spermatogenesis.

Results and Discussion

Expression of One miRNA Cluster Increases When the Other Cluster Is Inactivated. Using miRNA qPCR analyses, we examined the expression of all five miRNAs in 11 murine organs (Fig. 1*A*). Consistent with previous data (8), the testis displayed the most abundant expression of all five miRNAs (Fig. 1*A*). Other organs with detectable levels of more than one of the five miRNAs included ovary, brain, and lung. Inactivation of either the *miR-34b/c* or the *miR-449* cluster does not cause any discernible phenotype (8, 11, 12). Given the functional redundancy, it is likely that a lack of one of the two miRNA clusters could have been compensated for by the other cluster. To investigate the physiological roles of this miRNA family, we generated *miR-34b/c* and *miR-449* dKO mice (*SI Appendix*, Fig. S1). All five miRNAs in four organs of the dKO mice, including brain, testis, ovary, and lung, were absent, confirming complete inactivation of the two miRNA clusters (Fig. 1 *B*–*E*).

Intriguingly, levels of miR-449a and miR-449c were significantly increased in *miR-34b/c*–null brain, whereas levels of miR-34b and miR-34c were elevated in *miR-449*–null brain (Fig. 1*B*). Similar changes, but to a lesser extent, were observed in the testis of single KO mice (Fig. 1*C*). Increased expression of miR-449a/b/c, however, was observed in *miR-34b/c*–null ovaries and lungs, but there was no concomitant increase of miR-34b/c in *miR-449*–null ovaries and lungs (Fig. 1 *D* and *E*). This inverse relationship between the expression of one of the two miRNA clusters when

Significance

Most of the single miRNA gene knockouts display no developmental phenotype. Here, we report that simultaneous inactivation of two functionally overlapping miRNAs, *miR-34b/c* and *miR-449,* led to a sexually dimorphic partial perinatal lethality, growth retardation and sterility. Multiple underlying developmental defects, including underdevelopment of the basal forebrain structures, a lack of motile cilia in trachea and oviduct, severely disrupted spermatogenesis and oligoasthenoteratozoospermia, result from the dysregulation of ∼240 target genes that are mainly involved in three major cellular functions, including cell fate control, brain development and microtubule dynamics. This study provides physiological evidence demonstrating an essential role of *miR-34b/c* and *miR-449* in normal brain development, motile ciliogenesis and spermatogenesis.

Author contributions: C.X. and W.Y. designed research; J.W., J.B., M.K., S.Y., C.T., H.Z., and G.S.M. performed research; J.W., J.B., M.K., S.Y., C.T., H.Z., G.S.M., C.X., and W.Y. analyzed data; and W.Y. wrote the paper.

The authors declare no conflict of interest.

This article is a PNAS Direct Submission.

Freely available online through the PNAS open access option.

[1]J.B., M.K., S.Y., and C.T. contributed equally to this work.

[2]To whom correspondence may be addressed. E-mail: chenx@shsmu.edu.cn or wyan@medicine.nevada.edu.

This article contains supporting information online at www.pnas.org/lookup/suppl/doi:10.1073/pnas.1407777111/-/DCSupplemental.

DEVELOPMENTAL BIOLOGY

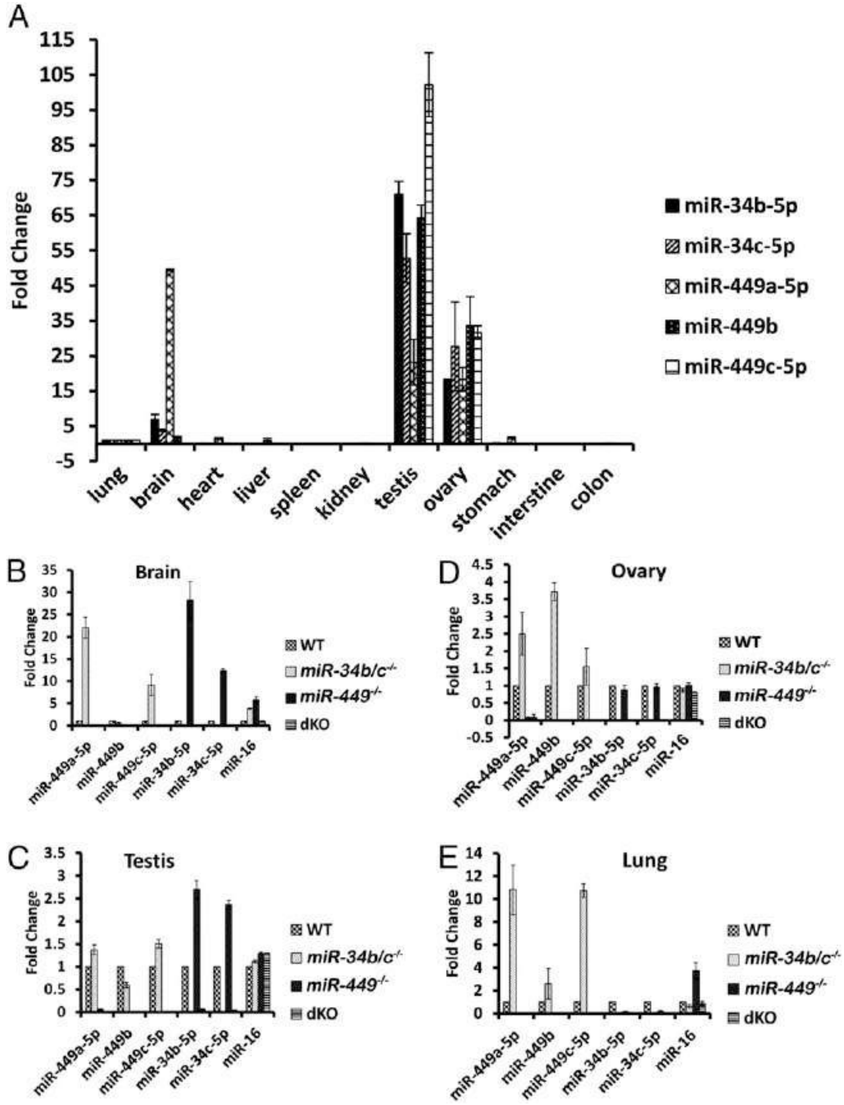

Fig. 1. Expression profiles of the five miRNAs (miR-34b, miR-34c, miR-449a, miR-449b, and miR-449c) encoded by the *miR-34b/c* and *miR-449* clusters in multiple organs of WT and KO mice. (*A*) Relative expression levels of the five miRNAs in 11 organs of WT mice. Expression levels of the five miRNAs were first determined using TaqMan-based qPCR analyses. Relative levels are represented by fold changes, which were calculated by designating the levels in lung as 1. Undetectable Ct values were considered no expression. (*B–E*) Fold changes in expression levels of the five miRNAs in single-KO (*miR-34b/c*$^{-/-}$ or *miR-449*$^{-/-}$) and double-KO (*miR-34*$^{-/-}$; *miR-449*$^{-/-}$) mice compared with the WT controls. Expression levels of the five miRNAs were first determined using TaqMan-based qPCR analyses, and fold changes were then calculated by designating the WT levels as 1. Four organs expressing the five miRNAs (*A*), including brain (*B*), testis (*C*), ovary (*D*), and lung (*E*), were analyzed. In miRNA qPCR analyses, U6 was used as a loading control, and values were calculated based on the relative quantification (ΔΔCt) method. All qPCR assays were performed in biological triplicates.

the other is inactivated may reflect a compensatory effect owing to their functional redundancy.

Sexually Dimorphic Partial Perinatal Lethality and Growth Retardation in dKO mice. Although single KO of either *miR-34b/c* or *miR-449* does not cause any abnormalities (8, 12), dKO mice tended to die at ∼postnatal day 7 (P7), and these dKO pups were grossly smaller than their double-heterozygous (*miR-34b/c*$^{+/-}$; *miR-449*$^{+/-}$) or "triple-negative" (*miR-34b/c*$^{-/-}$; *miR-449*$^{+/-}$ or *miR-34b/c*$^{+/-}$; *miR-449*$^{-/-}$) littermates (*SI Appendix*, Fig. S2). Analyzing the birth record of a total of 383 pups from the triple-negative breeding pairs (*SI Appendix*, Fig. S1), we found an average lethality rate of ∼46% for dKO mice (Fig. 2*A*). Notably, sexual dimorphism was observed between the dKO pups, with ∼57% of the male and ∼31% of the female dKO pups dying by ∼P7 (Fig. 2*A*). The lethality rate described above could have been greater had dKO pups not been transferred to foster mothers or had their normal littermates not been removed to improve the chance for dKO pups to feed. Therefore, the abnormal feeding behavior in dKO pups appeared to have contributed to the perinatal lethality phenotype. The dKO pups that survived beyond P7 did develop but generally were smaller than their double heterozygous or triple-negative littermates (*SI Appendix*, Fig. S2). Growth retardation was observed in dKO mice from P1 to P20, apparently more severe in the males than the females (Fig. 2*B* and *SI Appendix*, Table S1). However, the sexual dimorphism in growth retardation became less obvious after the dKO mice reached adulthood (Fig. 2*C* and *SI Appendix*, Fig. S2).

Brain Developmental Defects in dKO Mice. Given the abundant expression of the five miRNAs in brain, it is possible that complete ablation of these miRNAs led to defective brain development, which in turn caused the feeding defects, perinatal lethality, and growth retardation in dKO mice. Because the male dKO mice appeared to be more severe in the brain-related phenotype, we examined male dKO and control (double-heterozygous littermate) brains at embryonic day 18.5 (E18.5). In coronal and sagittal sections, the dKO basal forebrain structures appeared to be smaller compared with controls. In particular, sagittal sections of the E18.5 brains showed that the area of the olfactory tubercle (OT) was significantly smaller in dKO males compared with controls (55.8 ± 6.1% vs. 100%; $P < 0.005$, *t* test) (Fig. 3). The perinatal lethality phenotype in dKO mice is most likely caused by the brain defects, because the dKO mice all have smaller basal forebrain structures, including the caudate putamen (CPu) and the OT. The CPu and OT compose a large sector of the basal forebrain, broadly interconnected with many other brain regions, and are implicated in many functions, including reward pathways, feeding, and social

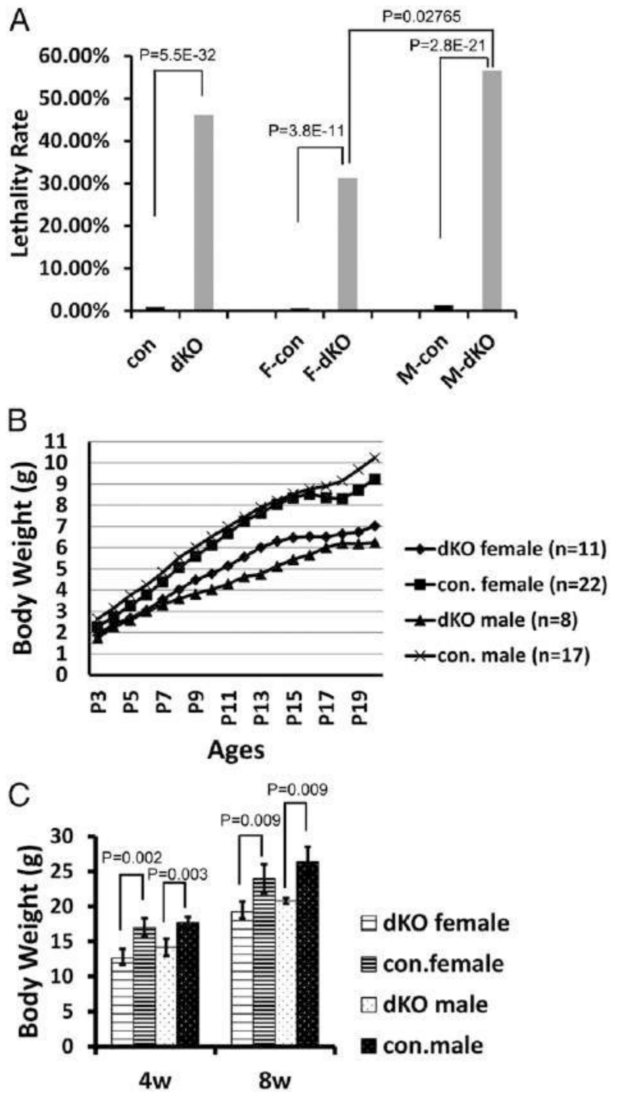

Fig. 2. Partial perinatal lethality and growth retardation in *miR-34b/c* and *miR-449* dKO mice. (*A*) Lethality rate of double heterozygous and "triple negative" (*miR-34b/c*$^{-/-}$; *miR-449*$^{+/-}$ or *miR-34b/c*$^{+/-}$; *miR-449*$^{-/-}$) littermate control (con) and *miR-34b/c–miR-449* dKO male (M) and female (F) pups around P7. *P* values < 0.01 are statistically significant. Data were based on 383 pups produced by triple-negative breeding pairs. (*B*) Growth curves showing the changes in body weight of double-heterozygous and triple-negative littermate control (con) and dKO male (M) and female (F) mice over the first 20 d of postnatal development (P1–P20). The number of pups (*n*) measured is indicated. Mean values are presented. Original mean values, SD, and *P* values are presented in *SI Appendix*, Table S1. (*C*) Body weight of control (con) and dKO male and dKO female mice at age 4 and 8 wk. Data are presented as mean ± SEM ($n = 6$). *P* values < 0.01 are statistically significant.

behaviors (13). The OT receives direct input from the olfactory bulb and also indirect input from the vomeronasal system accessory olfactory, which senses pheromone signals (13). The OT is also involved in dopamine signaling and the reward system, thereby linking odors with positive or negative emotions and motivations (13). Thus, the smaller olfactory tubercle may explain, as least in part, the feeding defects and the perinatal lethality phenotype in dKO mice.

Oligoasthenoteratozoospermia and Sterility in Male dKO Mice. Male dKO mice that survived to adulthood never produced pups when bred with fertility-proven WT adult females for 6 mo, suggesting that the dKO males are sterile. We performed gross and microscopic examination of the male reproductive organs of dKO mice (Fig. 4 and *SI Appendix*, Fig. S3). Significant differences were observed in the weight of the epididymis, but not of the testis or seminal vesicles (*SI Appendix*, Fig. S4). Testicular histological examination revealed that the adult (10 wk old) dKO seminiferous epithelia were severely atrophic and disorganized, with only one or two layers of spermatogenic cells lining the basal membrane of the seminiferous tubules (Fig. 4 *A–D*). A smaller number of sperm (~5–10% of that in WT) were recovered from the dKO epididymides (Fig. 4*E*), and these dKO sperm displayed minimal motility. Only ~2% of the dKO epididymal sperm showed normal morphology, compared with ~80% of sperm of normal morphology in WT males (Fig. 4 *F–H*). Resembling human oligoasthenoteratozoospermia (14), the dKO male mice displayed low sperm counts, low or no motility, and deformed sperm, which are most likely responsible for the male sterility phenotype. Defective meiotic progression can lead to severe germ cell depletion and thus low sperm counts, and spermiogenic disruptions usually lead to motility defects and/or sperm deformation (15). Considered together, the testicular disruptions closely correlate with the localization of the five miRNAs and likely represent the direct effects of the lack of the five miRNAs.

Infertility Due To Cilia-Less Oviducts in dKO Females. All dKO females were also infertile after breeding with fertility-proven WT males for 6 mo. Although follicular development appeared to be delayed between P10 and P30, likely arising from overall growth retardation, the number of developing follicles and corpora lutea in P60 dKO ovaries was comparable to that found in age-matched WT ovaries (Fig. 4*I* and *SI Appendix*, Fig. S4). Therefore, the delayed folliculogenesis might not be responsible for the infertility phenotype in dKO females. Further supporting this notion, superovulation experiments revealed that only 2–5 MII oocytes were retrieved from the oviducts of each of the dKO females after pregnant mare's serum gonadotropin (PMSG) and human chorionic gonadotropin stimulation, whereas ~50 MII oocytes were obtained from each of the age-matched WT females at P21, P35, or P56 (Fig. 4*J*). Examination of the postsuperovulation ovaries detected no discernible abnormalities in dKO vs. WT control ovaries (*SI Appendix*, Fig. S4), suggesting no defects in folliculogenesis and ovulation. Intriguingly, when we collected germinal vesicle (GV)-stage oocytes directly from dKO ovaries primed with PMSG, the number of GV-stage oocytes collected from dKO ovaries was similar to that collected from WT ovaries (Fig. 4*K*), and a 20-h culture in vitro led to a similar maturation rate from GV to meiosis I (MI) and meiosis II (MII) stages in WT and dKO oocytes (Fig. 4*L*). These findings strongly suggest that dKO ovaries can produce normal number of oocytes, and that ovulation can occur normally, but the ovulated oocytes cannot reach the ampulla region of the oviducts.

Given that the *miR-449* and *miR-34* miRNA clusters have been shown to be involved in ciliogenesis in *Xenopus* and zebrafish (16, 17), it is possible that the oviducts of the dKO females have defective cilia, resulting in failure to capture oocytes during ovulation or transport of ovulated oocytes to the ampulla region. Indeed, histological examination revealed that ciliated cells were rarely seen in the epithelia of the dKO oviducts, and that cilia were largely absent in dKO oviducts (Fig. 5 *A–D*). Thus, the lack of cilia in dKO oviduct epithelia is likely responsible for the female infertility phenotype, because ovulated oocytes fail to be captured, transported, or both to the ampulla region of the oviduct.

Underdeveloped Motile Cilia in Tracheal Epithelia. Motile cilia exist in the epithelia of two organs in mammals, the trachea and oviduct (18). Given the lack of cilia in dKO oviduct epithelia, we

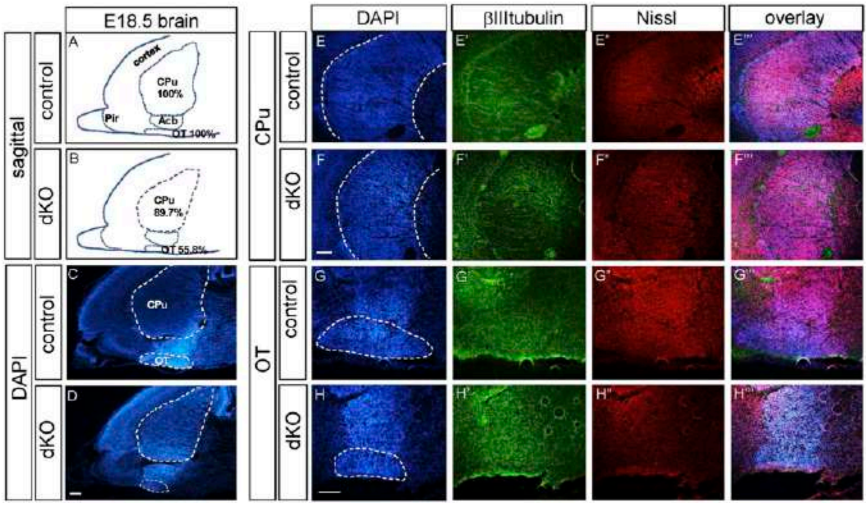

Fig. 3. Defects in basal forebrain structures in dKO mice. (*A* and *B*) Schematic diagram of the male basal forebrain at E18.5 showing differences in the area of the CPu and the OT between control and dKO brains. The dKO CPu area is ∼89.7% of the control, and the dKO OT is ∼55.8% of the control. (*C* and *D*) DAPI labeling of sagittal sections of the CPu at E18.5 showing that the dKO brains (n = 4) display narrow CPu regions and smaller OTs compared with control (n = 4). (Scale bars: 200 μm.) (*E*–*H*) High-magnification images of the control and dKO CPu and OT regions labeled with DAPI (*E*–*H*), βIII tubulin (*E*′–*H*′), and Nissl (*E*′′–*H*′′) in sagittal sections showing reduced size in the dKO brains compared with control. (Scale bars: 200 μm.) Pir, piriform cortex; Acb, accumbens nucleus.

examined the dKO trachea. We found that cilia were largely absent in the pseudostratified epithelia of the adult dKO trachea (Fig. 5 *E*–*H*). Motile cilia in the trachea are essential for cleansing mucus from the airway, and a lack of tracheal cilia should lead to obstruction of the airway (19). Thus, we examined the histology of the lung in more detail (*SI Appendix*, Fig. S5). The alveolar sacs in the lungs appeared to be drastically enlarged at P5 and P11 in dKO mice (*SI Appendix*, Fig. S5). Although this pathology appeared to persist into adulthood, the enlargement of the alveolar sacs became less obvious in dKO lungs compared

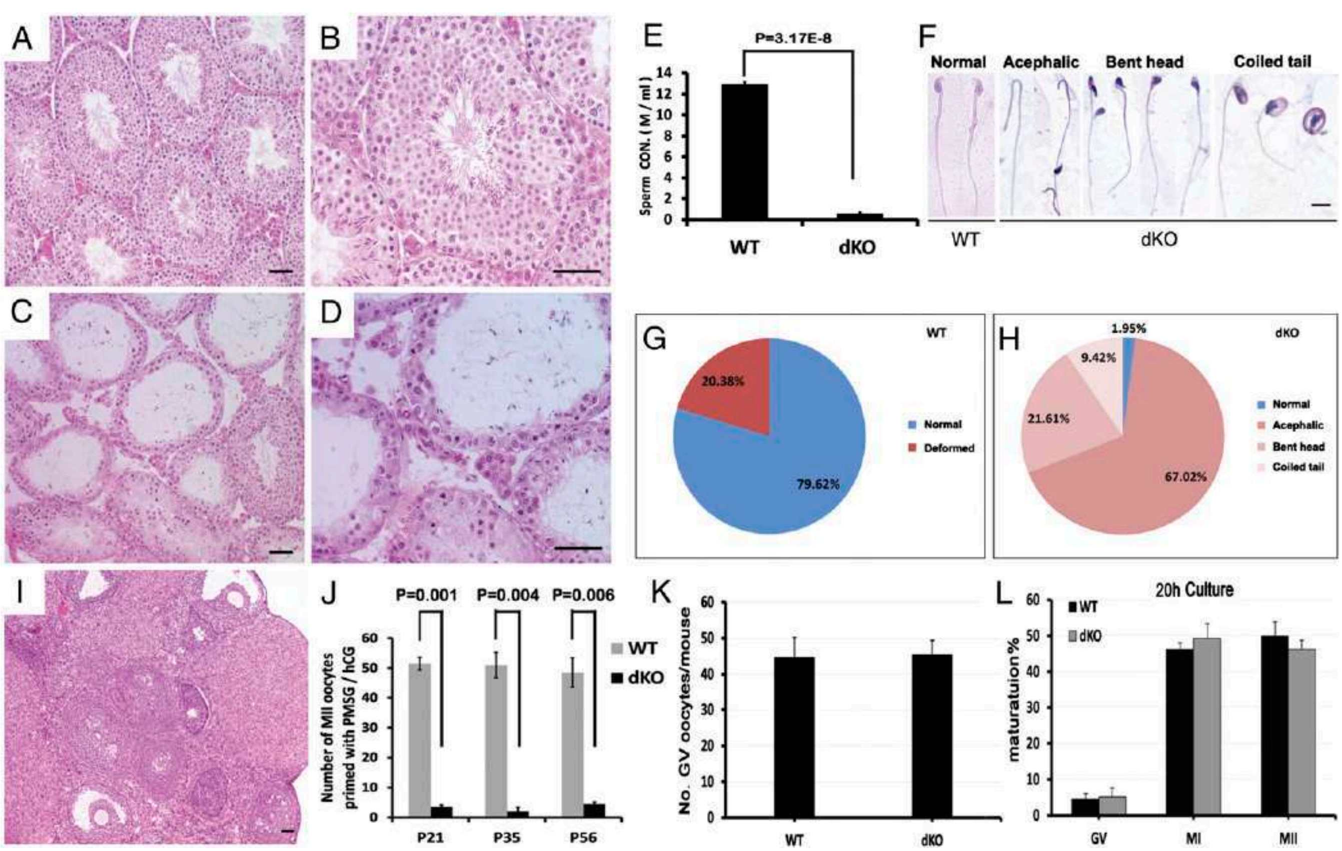

Fig. 4. Disrupted spermatogenesis and oligoasthenoteratozoospermia in male dKO mice, and oviduct defects in female dKO mice. (*A*–*D*) Testicular histology of 10-wk-old WT mice (*A* and *B*) and dKO mice (*C* and *D*). (Scale bar: 20 μm.) (*E*) Sperm counts of WT and dKO male mice. Data are presented as mean ± SEM (n = 6). (*F*) Deformed sperm in dKO male mice. (Scale bar: 20 μm.) (*G* and *H*) Pie charts showing the proportional distribution of normal and deformed sperm in WT (*G*) and dKO (*H*) male mice. (*I*) Normal ovarian histology of dKO female mice at P60. (Scale bar: 50 μm.) (*J*) Number of MII oocytes retrieved from the oviducts of adult WT and dKO female mice after superovulation. Data are presented as mean ± SEM (n = 6). (*K*) Number of germinal vesicle (GV)-stage oocytes retrieved from the PMSG-primed ovaries of adult WT and adult dKO female mice. Data are presented as mean ± SEM (n = 6). (*L*) Maturation rate of WT and dKO oocytes from GV to meiosis I (MI) and meiosis II (MII) stages during a 20-h culture in vitro. Data are presented as mean ± SEM (n = 6).

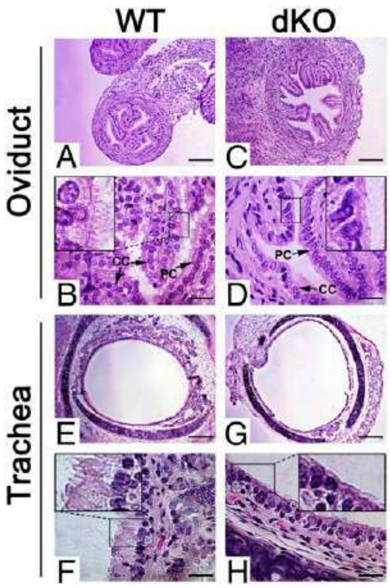

Fig. 5. Deficiency in motile ciliogenesis in dKO mice. (*A–D*) Although the WT oviduct epithelia consist of both Peg cells (PC) and ciliated cells (CC) with abundant cilia pointing to the lumen (*A* and *B*), CCs and cilia are rarely seen despite the presence of PCs in the epithelia of dKO oviducts (*C* and *D*). (*Insets*) Digitally enlarged, framed areas in *B* and *D*. (Scale bars: 200 μm in *A* and *C*, 20 μm in *B* and *D*.) Five WT and dKO mice were analyzed, and representative images are shown. (*E–H*) The pseudostratified columnar epithelia of the WT trachea contain abundant cilia pointing to the lumen (*E* and *F*), whereas cilia are largely lacking in the epithelia of the dKO trachea (*G* and *H*). (*Insets*) Digitally enlarged and framed areas in *F* and *H*. (Scale bars: 200 μm in *E* and *G*, 20 μm in *F* and *H*). Five WT and dKO mice were analyzed, and representative images are shown.

with WT control lungs (*SI Appendix*, Fig. S5). Because mucus cleansing is critical for the respiratory functions in perinatal development, the lack of cilia in the trachea may contribute to perinatal lethality, as well as to feeding defects related to aberrant basal forebrain development.

Dysregulation of 239 Genes Directly Targeted by the Five miRNAs Are Responsible for the Developmental Defects in dKO Mice. Because miRNAs function mainly by affecting mRNA stability (20), we attempted to identify the target genes for the five miRNAs using an unbiased approach, RNA-Seq–based transcriptomic analyses followed by Sylamer analyses (21). A total of 2,863, 3,427, and 4,123 genes were dysregulated in dKO male brains, female brains, and testes, respectively (*SI Appendix*, Table S2). We performed Sylamer analyses to identify the miRNAs responsible for the dysregulated mRNAs (21). In general, the enriched seed sequences ("words with the highest peak") were not that of the five miRNAs (*SI Appendix*, Figs. S6 and S7).

These data imply that the transcriptomic changes observed in those dKO organs most likely represent secondary effects. This idea is plausible, given that the organs were analyzed at P10, after the developmental defects apparently had persisted for quite some time; for example, the brain defects in dKO mice became obvious as early as E18.5 (Fig. 3). Therefore, we adopted an alternative approach by analyzing miRNA targets predicted by TargetScan (22–25) among dysregulated genes in the RNA-Seq data. Among the dysregulated mRNAs, the majority of target genes were up-regulated in male brain and testis samples (83–88%; *SI Appendix*, Table S3), suggesting a direct effect on target mRNA stability in the absence of the five miRNAs.

The RNA-Seq data were further validated by qPCR analyses, which demonstrated that most of the 44 representative genes displayed similar up- or down-regulation between qPCR and RNA-Seq analyses (*SI Appendix*, Fig. S8). GO term enrichment analyses classified the dysregulated genes into three major functional groups: cell fate control, brain development, and cytoskeleton organization (Fig. 6). Notably, 239 (*SI Appendix*, Table S2) out of 439 targets (*SI Appendix*, Table S4), including both predicted and validated, for the five miRNAs were mostly up-regulated in dKO brain and testis (*SI Appendix*, Table S3). GO term enrichment analyses of the dysregulated mRNAs targeted by the five miRNAs revealed that these mRNAs were also classified into the same three major functional groups as the globally dysregulated mRNAs (*SI Appendix*, Fig. S9). These data indicate that the transcriptomic changes detected by RNA-Seq analyses result from dysregulation of the direct targets of the five miRNAs as well as their downstream genes involved in three major cellular functions: cell fate control, brain development, and cytoskeleton organization.

Among the dysregulated genes enriched in the three major GO terms, ∼4–5% were identified as direct targets of the five miRNAs (Fig. 6 and *SI Appendix*, Tables S2 and S3 and Datasets S1–S3), further supporting that the phenotypes observed mostly represent the effects secondary to the primary defects caused by ablation of the five miRNAs during early development. Moreover, disrupted cellular processes identified by GO term enrichment analyses appear to correlate closely with the phenotypes observed in dKO mice; for example, genes involved in cytoskeletal organization/microtubule dynamics were enriched among the dysregulated genes (Fig. 6 and *SI Appendix*, Table S2 and Datasets S1–S3), correlating closely with the impaired motile ciliogenesis. Overall, our unbiased mRNA profiling and GO term enrichment analyses support our tenet that the majority of the predicated target genes are truly the targets for the five miRNAs under physiological conditions, and that all of the multiple phenotypes observed—including aberrant brain development, defective motile ciliogenesis, and disrupted spermatogenesis—result from dysregulation of their direct targets as well as their downstream genes.

In summary, our work reveals an essential role of two miRNA clusters, *miR-34b/c* and *miR-449*, in normal brain development, motile ciliogenesis, and spermatogenesis. Further characterization may reveal more subtle defects, and detailed molecular analyses will define gene networks responsible for the critical developmental processes controlled by the two miRNA clusters.

Materials and Methods

Generation of *miR-34b/c* and *miR-449* dKO Mice. miRNA dKO mice were generated by breeding *miR-34b/c*$^{-/-}$ mice with *miR-449*$^{-/-}$ mice (8, 12). Details are provided in *SI Appendix, Materials and Methods*.

Small RNA Isolation and qPCR Analyses. Small RNAs were isolated from different murine organs using the mirVana miRNA isolation kit (Ambion) according to the manufacturer's instructions. Details are provided in *SI Appendix, Materials and Methods*.

mRNA Isolation and qPCR Analyses. Total RNA was isolated using TRIzol reagent (Invitrogen) according to the manufacturer's instructions. qPCR analyses were performed as described previously (26).

Histology and Immunohistochemistry. Histological analyses were performed as described previously (26). Preparation of the brain samples and immunofluorescent staining of βIII tubulin and NISSL were done as described previously (27, 28).

RNA-Seq and Bioinformatic Analyses. RNA-Seq was performed using an Illumina HiSEq. 2000 sequencer (100-bp paired-end reads). RNA-Seq data were processed using Tophat (29) and Cufflinks (30) following a published protocol (31). Ingenuity (Qiagen) was used to analyze Gene Ontology terms.

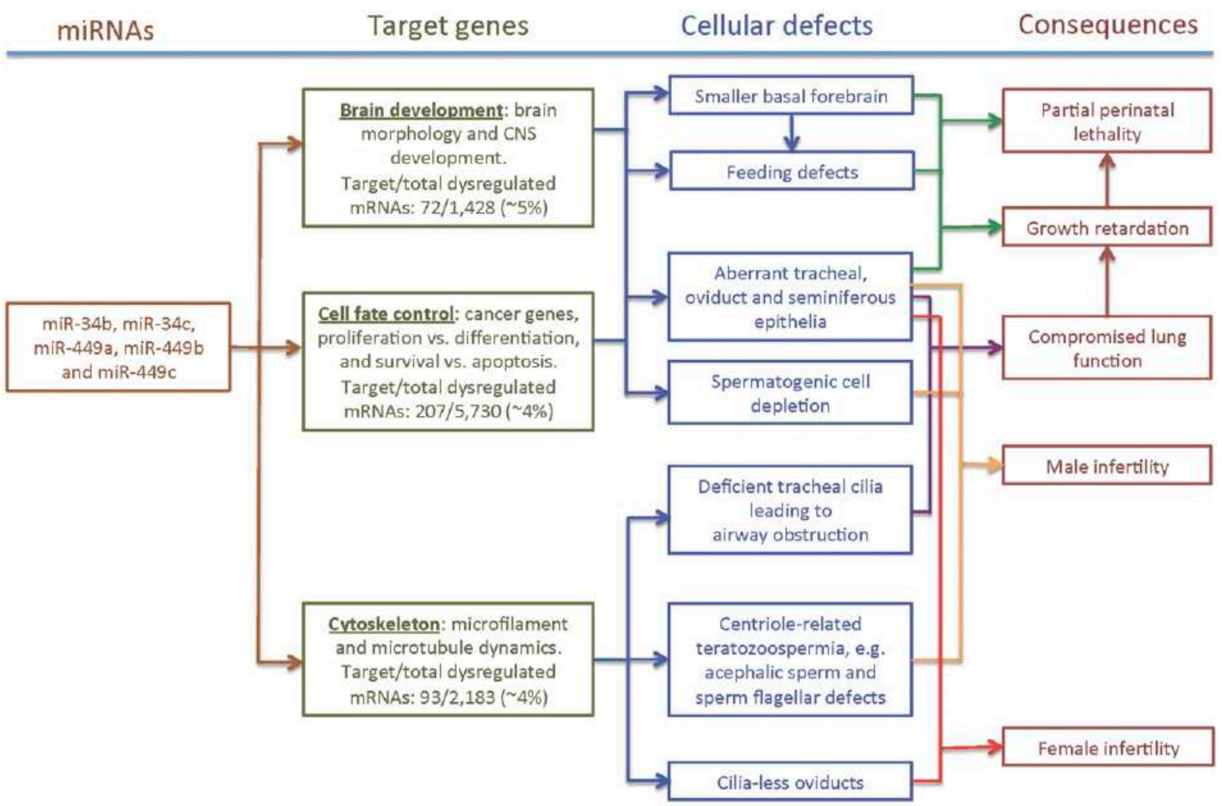

Fig. 6. GO term enrichment analyses. Analyses of dysregulated genes in dKO brains and testes reveal that the five miRNAs control 239 target mRNAs involved in three major cellular functions, including brain development, cell fate control, and cytoskeleton dynamics. Disrupted brain development, motile ciliogenesis, and spermatogenesis in dKO mice result from both the primary and secondary effects of dysregulated target genes, owing to ablation of the five miRNAs.

miRNA target genes were determined using TargetScan (22–25), and only predictions with conserved sites were considered. Sylamer analyses were also performed as described previously (21). Details are provided in *SI Appendix, Materials and Methods*.

Statistics. For bioinformatic analyses, pipeline-specific statistical methods were used as described previously (21, 29–31). χ^2-test was used for analyzing the data on perinatal lethality rate. Student *t* test was adopted for the rest of statistic analyses.

ACKNOWLEDGMENTS. We thank Dr. Lin He, University of California Berkeley, for providing the *miR-34b/c* KO mice. This work was supported in part by National Institutes of Health (NIH) Grants HD060858, HD071736, and HD074573 (to W.Y.) and NS077169 (to G.S.M.); National Natural Science Foundation of China Grants 30771139 (to C.X.) and 31270029 (to J.W.); and Shanghai Natural Science Foundation Grant 12JC1405500 (to C.X.). All KO mouse lines were generated and maintained in the University of Nevada Genetic Engineering Center, supported by NIH COBRE Grant P20-RR18751. Further support for core facilities was provided by NIH Grants P20-RR016464, P20-GM103440, P20-GM103554, and P20-GM103650.

1. Bartel DP (2009) MicroRNAs: Target recognition and regulatory functions. *Cell* 136(2): 215–233.
2. Bartel DP (2004) MicroRNAs: Genomics, biogenesis, mechanism, and function. *Cell* 116(2):281–297.
3. Loh YH, Yi SV, Streelman JT (2011) Evolution of microRNAs and the diversification of species. *Genome Biol Evol* 3:55–65.
4. Janga SC, Vallabhaneni S (2011) MicroRNAs as post-transcriptional machines and their interplay with cellular networks. *Adv Exp Med Biol* 722:59–74.
5. Peters J, Robson JE (2008) Imprinted noncoding RNAs. *Mamm Genome* 19(7-8): 493–502.
6. Schmitt MJ, Margue C, Behrmann I, Kreis S (2013) MiRNA-29: A microRNA family with tumor-suppressing and immune-modulating properties. *Curr Mol Med* 13(4): 572–585.
7. Wong KY, Yu L, Chim CS (2011) DNA methylation of tumor suppressor miRNA genes: A lesson from the miR-34 family. *Epigenomics* 3(1):83–92.
8. Bao J, et al. (2012) MicroRNA-449 and microRNA-34b/c function redundantly in murine testes by targeting E2F transcription factor-retinoblastoma protein (E2F-pRb) pathway. *J Biol Chem* 287(26):21686–21698.
9. Lizé M, Klimke A, Dobbelstein M (2011) MicroRNA-449 in cell fate determination. *Cell Cycle* 10(17):2874–2882.
10. Lizé M, Pilarski S, Dobbelstein M (2010) E2F1-inducible microRNA 449a/b suppresses cell proliferation and promotes apoptosis. *Cell Death Differ* 17(3):452–458.
11. Concepcion CP, et al. (2012) Intact p53-dependent responses in miR-34–deficient mice. *PLoS Genet* 8(7):e1002797.
12. Choi YJ, et al. (2011) miR-34 miRNAs provide a barrier for somatic cell reprogramming. *Nat Cell Biol* 13(11):1353–1360.
13. Wesson DW, Wilson DA (2011) Sniffing out the contributions of the olfactory tubercle to the sense of smell: Hedonics, sensory integration, and more? *Neurosci Biobehav Rev* 35(3):655–668.
14. Cavallini G (2006) Male idiopathic oligoasthenoteratozoospermia. *Asian J Androl* 8(2): 143–157.
15. Yan W (2009) Male infertility caused by spermiogenic defects: Lessons from gene knockouts. *Mol Cell Endocrinol* 306(1-2):24–32.
16. Marcet B, et al. (2011) Control of vertebrate multiciliogenesis by miR-449 through direct repression of the Delta/Notch pathway. *Nat Cell Biol* 13(6):693–699.
17. Wang L, et al. (2013) miR-34b regulates multiciliogenesis during organ formation in zebrafish. *Development* 140(13):2755–2764.
18. Mitchell DR (2007) The evolution of eukaryotic cilia and flagella as motile and sensory organelles. *Adv Exp Med Biol* 607:130–140.
19. Marshall WF, Nonaka S (2006) Cilia: Tuning in to the cell's antenna. *Curr Biol* 16(15): R604–614.
20. Guo H, Ingolia NT, Weissman JS, Bartel DP (2010) Mammalian microRNAs predominantly act to decrease target mRNA levels. *Nature* 466(7308):835–840.
21. van Dongen S, Abreu-Goodger C, Enright AJ (2008) Detecting microRNA binding and siRNA off-target effects from expression data. *Nat Methods* 5(12):1023–1025.
22. Friedman RC, Farh KK, Burge CB, Bartel DP (2009) Most mammalian mRNAs are conserved targets of microRNAs. *Genome Res* 19(1):92–105.
23. Garcia DM, et al. (2011) Weak seed-pairing stability and high target-site abundance decrease the proficiency of lsy-6 and other microRNAs. *Nat Struct Mol Biol* 18(10): 1139–1146.
24. Grimson A, et al. (2007) MicroRNA targeting specificity in mammals: Determinants beyond seed pairing. *Mol Cell* 27(1):91–105.

25. Lewis BP, Burge CB, Bartel DP (2005) Conserved seed pairing, often flanked by adenosines, indicates that thousands of human genes are microRNA targets. *Cell* 120(1):15–20.
26. Wu Q, et al. (2012) The RNase III enzyme DROSHA is essential for microRNA production and spermatogenesis. *J Biol Chem* 287(30):25173–25190.
27. Dugan JP, Stratton A, Riley HP, Farmer WT, Mastick GS (2011) Midbrain dopaminergic axons are guided longitudinally through the diencephalon by Slit/Robo signals. *Mol Cell Neurosci* 46(1):347–356.
28. Nural HF, Mastick GS (2004) Pax6 guides a relay of pioneer longitudinal axons in the embryonic mouse forebrain. *J Comp Neurol* 479(4):399–409.
29. Trapnell C, Pachter L, Salzberg SL (2009) TopHat: Discovering splice junctions with RNA-Seq. *Bioinformatics* 25(9):1105–1111.
30. Trapnell C, et al. (2010) Transcript assembly and quantification by RNA-Seq reveals unannotated transcripts and isoform switching during cell differentiation. *Nat Biotechnol* 28(5):511–515.
31. Trapnell C, et al. (2013) Differential analysis of gene regulation at transcript resolution with RNA-seq. *Nat Biotechnol* 31(1):46–53.

SI Appendix*

Two miRNA clusters, *miR-34b/c* and *miR-449*, are essential for normal brain development, motile ciliogenesis and spermatogenesis

Jingwen Wu[a,b,c], Jianqiang Bao[a*], Minkyung Kim[d*], Shuiqiao Yuan[a*], Chong Tang[a*], Huili Zheng[a], Grant S. Mastick[d], Chen Xu[b,c] and Wei Yan[a]

[a]Department of Physiology and Cell Biology, University of Nevada School of Medicine, Reno, NV 89557, USA; [b]Department of Histology and Embryology, Shanghai Jiao Tong University School of Medicine, Shanghai 200025, China; [c]Shanghai Key Laboratory of Reproductive Medicine, Shanghai 200025, China; [d]Department of Biology, University of Nevada, Reno, Reno, NV 89557, USA.

*This file contains SI Materials and Methods, Figs. S1-S9 and Tables S1-S6.

SI Materials and Methods

Mouse Breeding. The Institutional Animal Care and Use Committee (IACUC) of the University of Nevada, Reno, approved all animal work. Mice were housed and maintained under specific pathogen-free conditions with a temperature- and humidity-controlled animal facility in the University of Nevada, Reno. *miR-449* and *miR-34b/c* knockout mice were generated as described (1, 2). All mice used in this study were on the C57BL/6J background. *miR-449*$^{-/-}$ and *miR-34bc*$^{-/-}$ mice were used to generate double knockout (*miR-449*$^{-/-}$;*miR-34bc*$^{-/-}$) mice using a breeding scheme as illustrated in Fig. S1. To enhance the survival rate of dKO pups, double heterozygous or “triple-negative” littermates were removed to foster mothers as soon as the dKO pups were identified based on their smaller size, which was usually around P3-P5.

Small RNA isolation and qPCR analyses. Small RNAs were isolated from different murine organs using the mirVana miRNA isolation kit (Ambion) according to the manufacturer’s instructions. For miRNA real-time qPCR, a TaqMan® MicroRNA Assay Kit (Applied Biosystems) was used, including the following assays: miR-449a (Assay ID: 001030), miR-449b (Assay ID: 002539), miR-449c (Assay ID: 001667), miR-34b (Assay ID: 002617), miR-34c (Assay ID: 000428), and miR-16 (Assay ID: 000391). All quantitative real-time PCR runs were carried out according to manufacturer’s instructions. U6 snRNA (Assay ID: 001973) was used for normalization. All PCR reactions were performed in triplicate. Primer sequences are listed in Table S5.

Collection of GV and MII oocytes through superovulation. Both WT and dKO female mice at P21, P35 and P56 were primed with pregnant mare's serum gonadotropin (PMSG, 5IU/mouse) *via* intraperitoneal injection (*i.p.*). The primed mice were sacrificed 46-48h after PMSG treatment, and the ovaries were dissected in M2 medium to release GV stage oocytes. For mature (MII stage) oocytes, mice were first injected with PMSG (5IU/mouse, *i.p.*) and subsequently with human chorionic gonadotropin (hCG) (5IU/mouse, *i.p.*) 48h after PMSG treatment, followed by collecting MII stage oocytes with cumulus cells from oviduct 14-16h after hCG treatment.

RNA-Seq. Large RNA was isolated from WT and dKO brains and testes at P10 using the mirVana RNA isolation kit (Ambion) according to the manufacturer’s instructions. All samples are in biological triplicates. RNA quality and quantity were assessed using the Agilent 2100 Bioanalyzer. RNA samples were sent to the UCLA Neuroscience Genomic Core for sequencing. Each library was sequenced for three times using an Illumina HiSeq 2000 sequencer (100bp paired-end reads).

Bioinformatic analyses of the RNA-Seq data. RNA-Seq data were processed using Tophat (3) and Cufflinks (4) following a published protocol (5). Ingenuity (Qiagen) was employed to analyze gene ontology terms with a cut off set at $p<0.1$ (one-way t-test). Target genes of the five miRNAs were determined using the Bioconductor Package-targetscan.Mm.eg.db (citation ("targetscan.Mm.eg.db") (6). Sylamer analyses were conducted as described (7). In brief, the cuffdiff-processed RNA differential expression data were processed by using cutoff p-value≤0.05. The significantly dysregulated genes were arranged by the order of fold change, and UTR data were obtained through the bioconductor package "Genomicranges". The arranged datasets were then processed using Sylamer and the settings were the same as those used in the *miR-155* knockout mouse study (7).

High-throughput real time quantitative PCR (HT-qPCR). Total RNA was extracted from tissues using mirVana miRNA Isolation Kit (Ambion, Cat#. AM1560). Large and small RNA portions were fractionated according to manufacturer's protocol, followed by the DNase treatment to remove potential genomic DNA contamination. First strand cDNA was synthesized using SuperScript® III First-Strand Synthesis System kit (Invitrogen, Catalog Number 18080-051), and all cDNA samples were adjusted to the same concentration at 60ng/μl prior to specific target amplification (STA). Each reaction for STA contained a 5μl volume of mixture of the following reagents: 2.5μl 2×TaqMan PreAmp Master mix (Invitrogen), 0.5μl 500nM pooled primer mix, 0.75μl distilled water and 1.25μl cDNA sample. The samples were programmed in a conventional PCR machine using 12 cycles of amplification, followed by Exonuclease I treatment to remove potential excess primers. The recovered cDNA samples were 7-fold diluted for subsequent fluorescent dye (EvaGreen)-based qPCR amplification on a Fluidigm Biomark HD system (Fluidigm). For qPCR analyses, 5μl sample mixture containing 2.5μl TaqMan gene expression master mix (2×), 0.25μl DNA-binding dye sample loading reagent (20×), 0.25μl EvaGreen DNA-binding dye (20×) and 2μl diluted cDNA sample, as well as 5μl assay mixture containing 2.5μl assay loading reagent (2×) and 2.5μl primer pairs (10μM) were loaded into inlets of a 48×48 Biomark chip (Fluidigm). The following program was setup for qPCR reaction: 10min at 25°C for thermal mixing, 2 min at 50°C for Uracil-N-glycosylase activation, 10min at 95°C for hot start activation of Taq polymerase, 35 cycles of 15 sec denature at 95°C and 1 min of annealing and elongation step at 60°C, followed by a melting curve temperature setup from 60°C to 95°C. Data were acquired and analyzed by Fluidigm Real-Time PCR Analysis Software v 3.0. Relative gene expression values were calculated based on ΔΔCt method as described before. Primer sequences are listed in Table S6.

References

1. Bao J*, et al.* (2012) MicroRNA-449 and microRNA-34b/c function redundantly in murine testes by targeting E2F transcription factor-retinoblastoma protein (E2F-pRb) pathway. *The Journal of biological chemistry* 287(26):21686-21698.
2. Choi YJ*, et al.* (2011) miR-34 miRNAs provide a barrier for somatic cell reprogramming. *Nature cell biology* 13(11):1353-1360.
3. Trapnell C, Pachter L, & Salzberg SL (2009) TopHat: discovering splice junctions with RNA-Seq. *Bioinformatics* 25(9):1105-1111.
4. Trapnell C*, et al.* (2010) Transcript assembly and quantification by RNA-Seq reveals unannotated transcripts and isoform switching during cell differentiation. *Nature biotechnology* 28(5):511-515.
5. Trapnell C*, et al.* (2013) Differential analysis of gene regulation at transcript resolution with RNA-seq. *Nature biotechnology* 31(1):46-53.
6. Krek A*, et al.* (2005) Combinatorial microRNA target predictions. *Nature genetics* 37(5):495-500.
7. van Dongen S, Abreu-Goodger C, & Enright AJ (2008) Detecting microRNA binding and siRNA off-target effects from expression data. *Nature methods* 5(12):1023-1025.

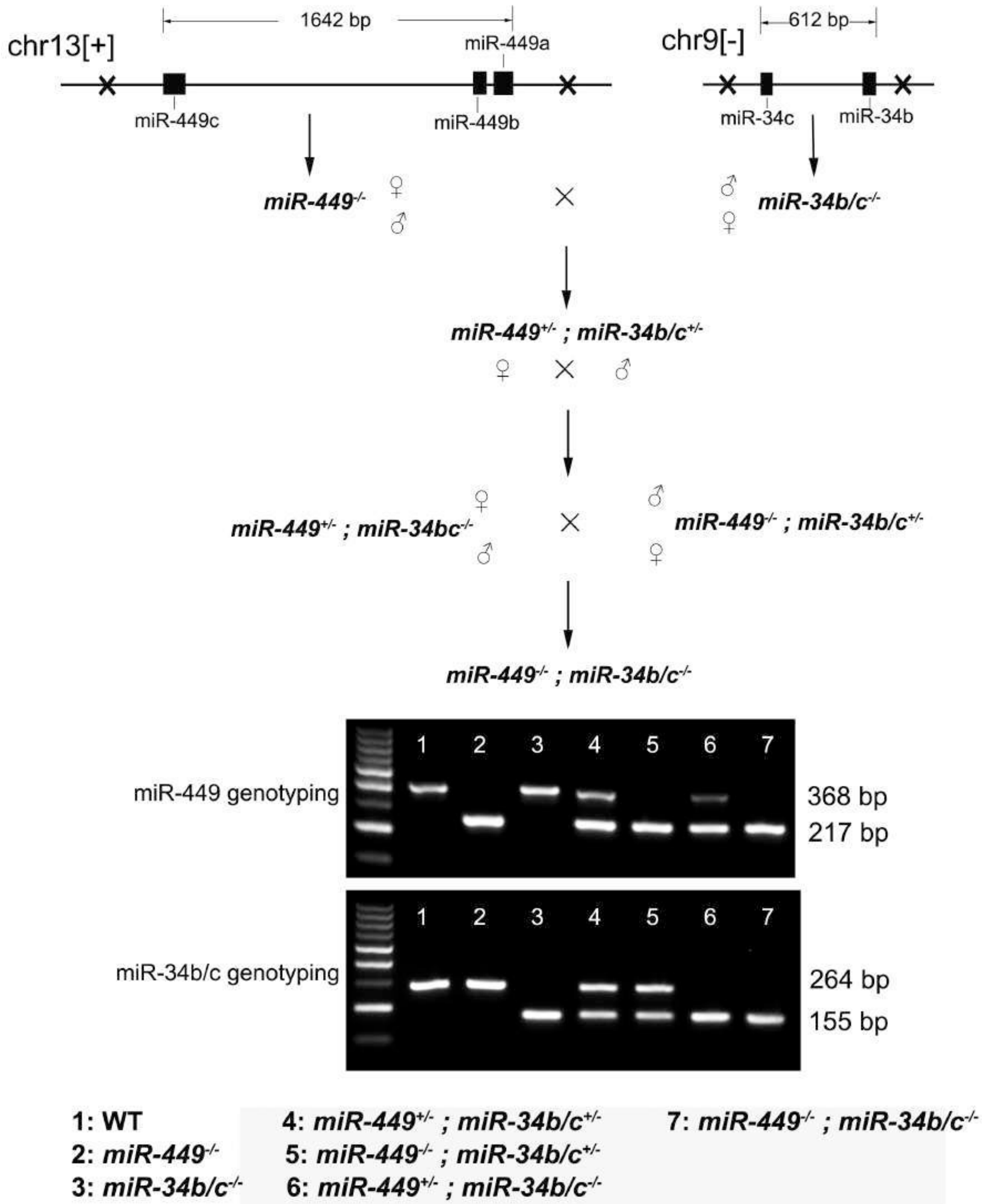

Figure S1. Breeding strategy and genotyping analyses for *miR-34b/c* and *miR-449* double knockout mice.

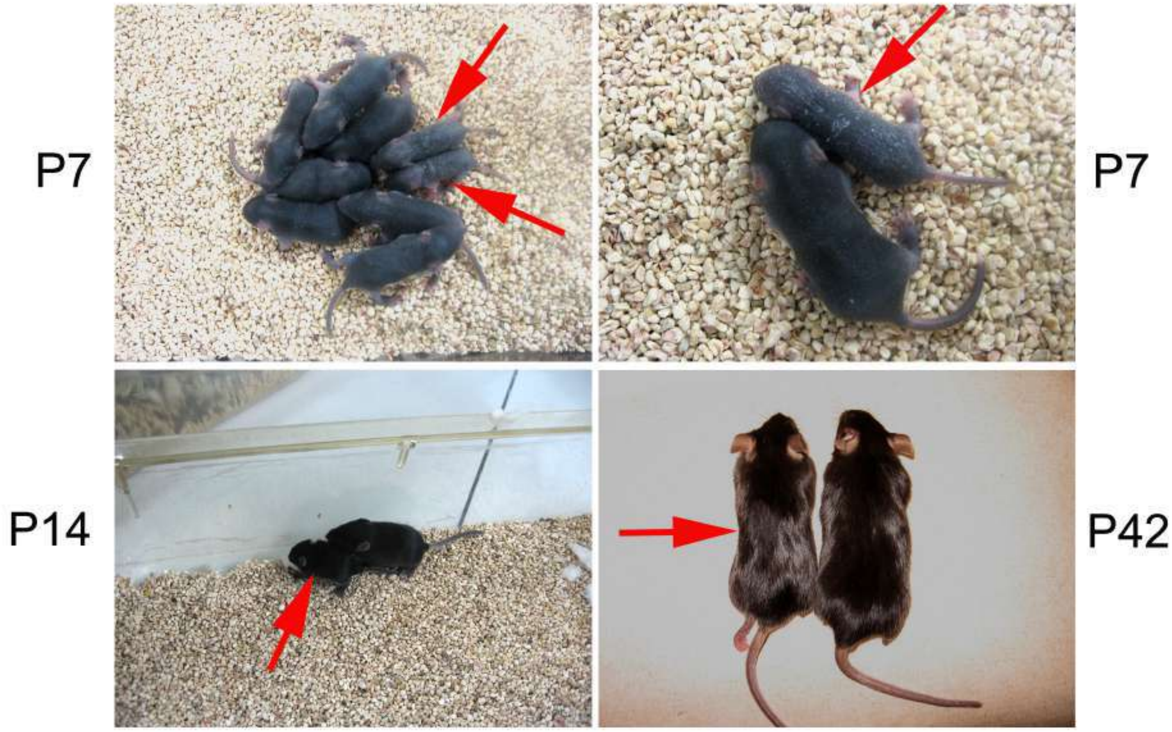

Figure S2. *miR-34b/c* and *miR-449* double knockout (dKO) mice are smaller in size during postnatal development (e.g., at P7 and P14) and the size difference becomes less obvious in adulthood (e.g., at P42). Arrows point to dKO mice.

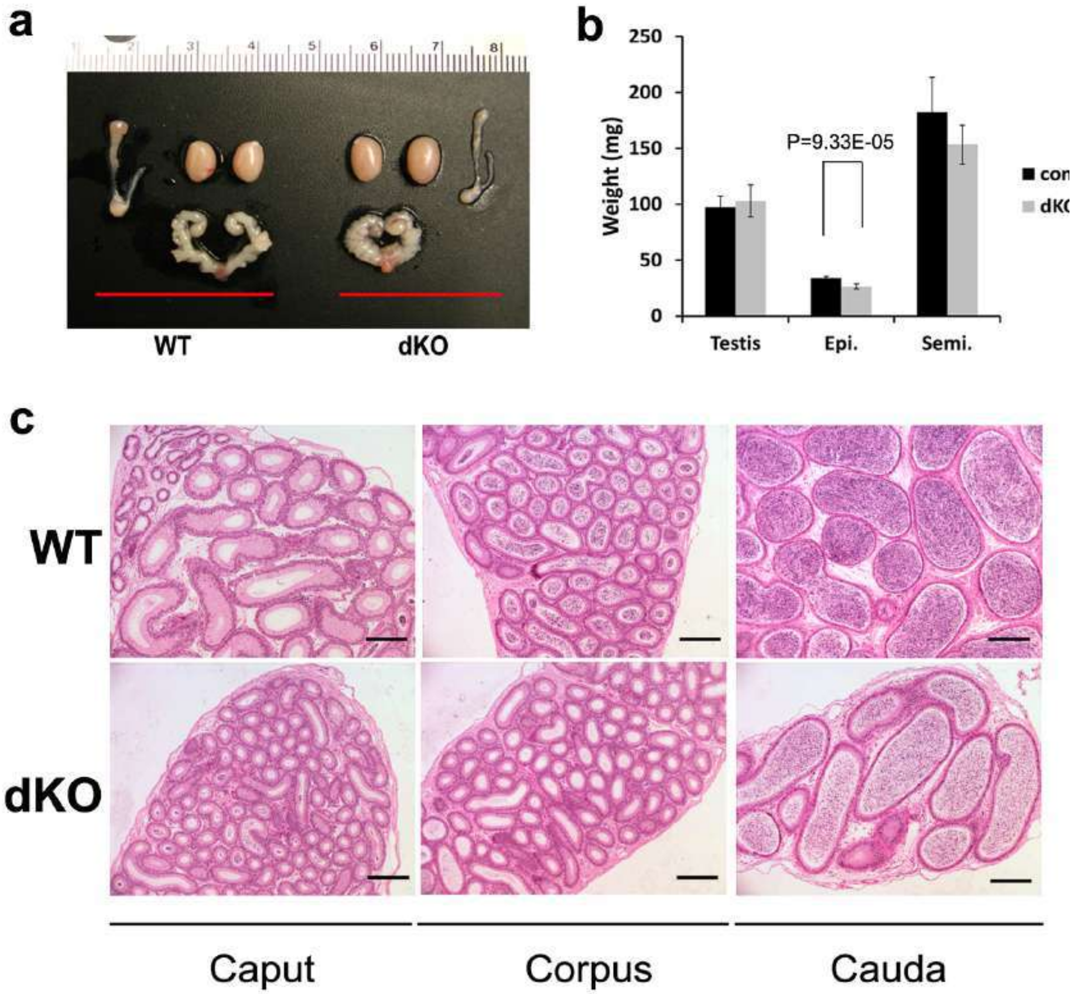

Figure S3. Gross morphology, weight of major reproductive organs, and epididymal histology in adult WT and dKO males. (**a**) Gross morphology of the testis, epididymis, and seminal vesicle of adult WT and dKO males. Nine adult WT and dKO male mice were analyzed and representative images are shown. (**b**) Mass of the testis, epididymis, and seminal vesicle of adult WT and dKO male mice. Significant differences were observed between WT and dKO epididymides. Data are presented as mean ± SEM (n=9). (**c**) Epididymal histology of adult WT and dKO mice. Scale bar = 400μm. Nine adult WT and dKO male mice were analyzed and representative images are shown.

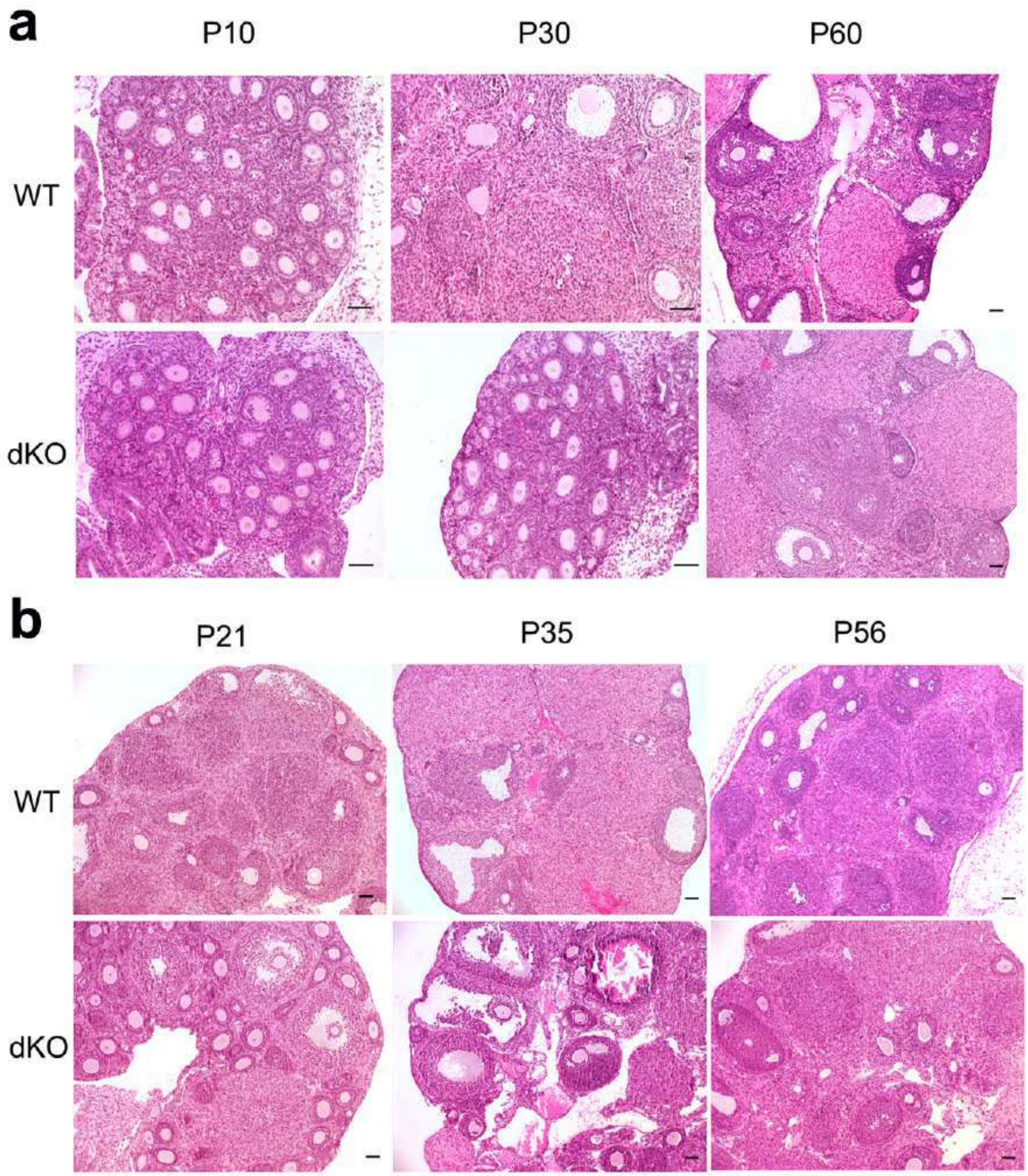

Figure S4. Ovarian histology of WT and dKO female mice. (**a**) Ovarian histology of WT and dKO female mice at P10, P30, and P60. (**b**) Post-superovulation ovarian histology of WT and dKO female mice at P21, P35, and P56. Scale bar = 200μm. Four WT and dKO mice at each of the six age groups were analyzed and representative images are shown.

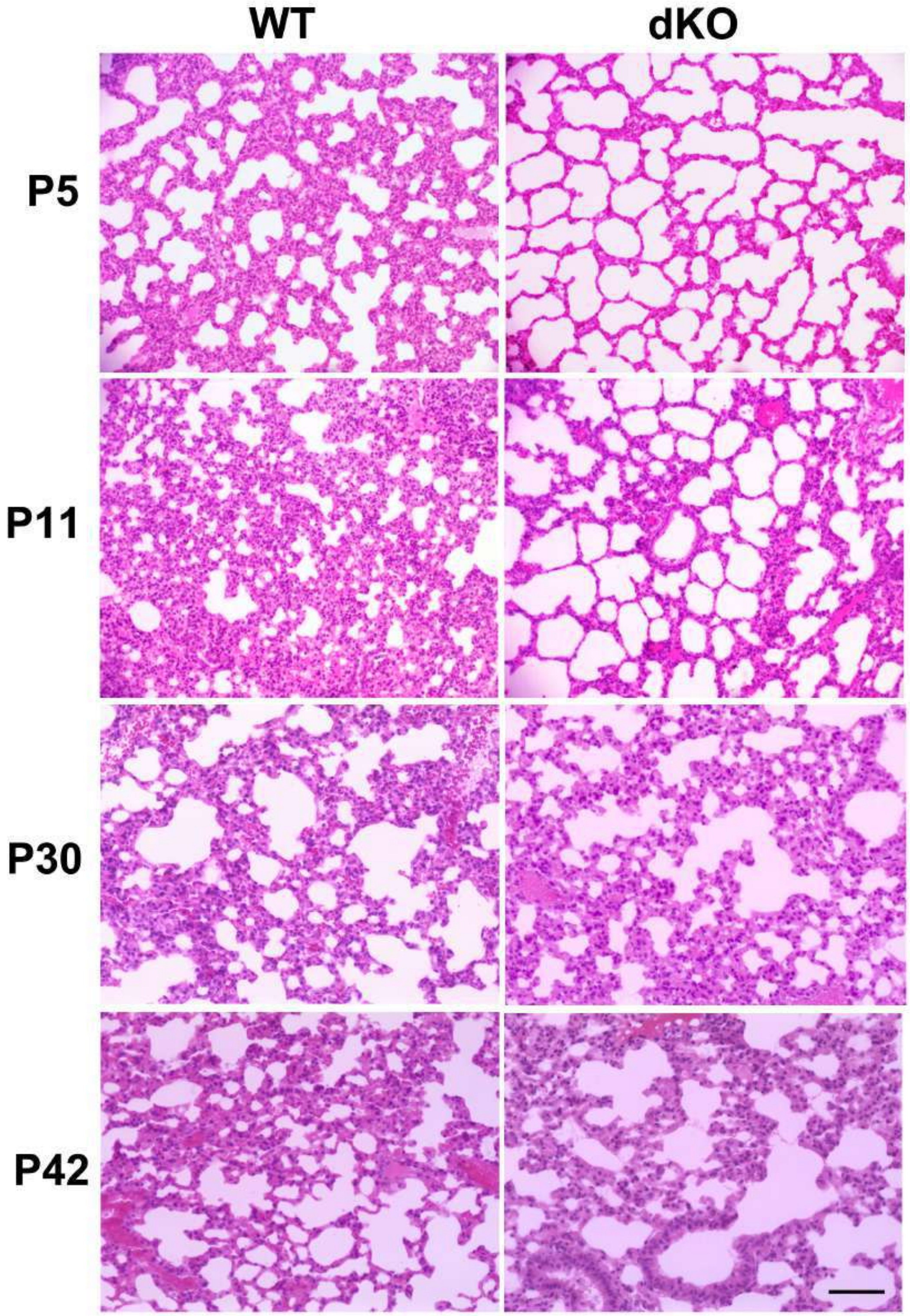

Figure S5. Histology of developing lungs in WT and dKO male mice at postnatal day 5 (P5), P11, P30, and P42. Note the enlarged alveolar sacs (*) in dKO mice that died at P5 and P11. Images of all panels were taken with the same magnification. Scale bar =100μm. Six WT and dKO mice at each of the four age groups were analyzed and representative images are shown.

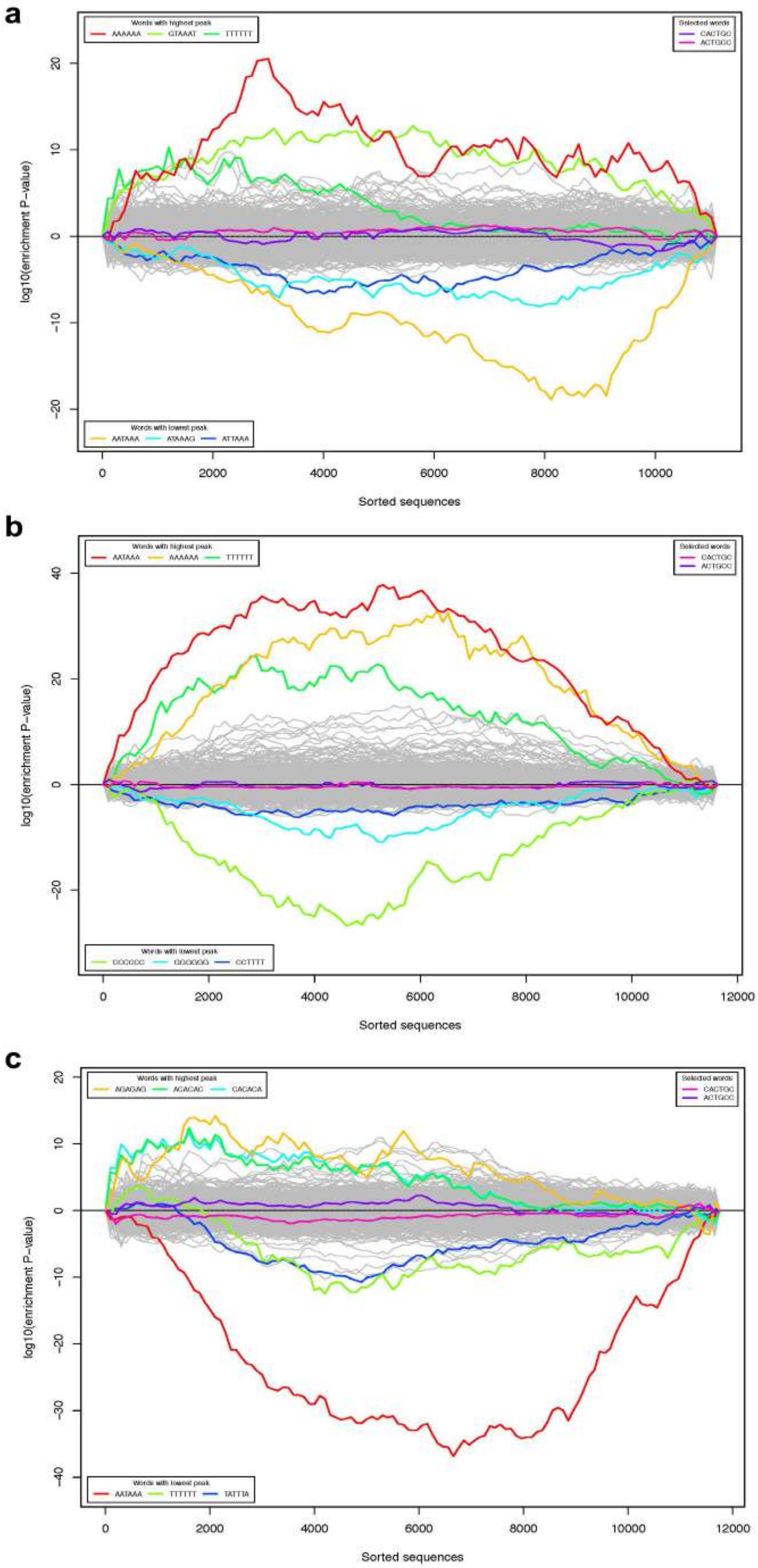

Figure S6. Sylamer analyses of the dysregulated mRNAs in male brains (a), female brains (b) and testes (c) of dKO mice at postnatal day 10. Since the five miRNAs (miR-34b, miR-34c, miR-449a, miR-449b and miR-449c) share the same seed sequence of “GGCAGUG”, we analyzed two possible 6nt seed sequence combinations, including one with the 1st-6th nt and the other with the 2nd-7th nt (“selected words”). The results suggest that the changes in mRNA transcriptome are likely caused by secondary effects due to dysregulation of miRNA direct targets in dKO organs.

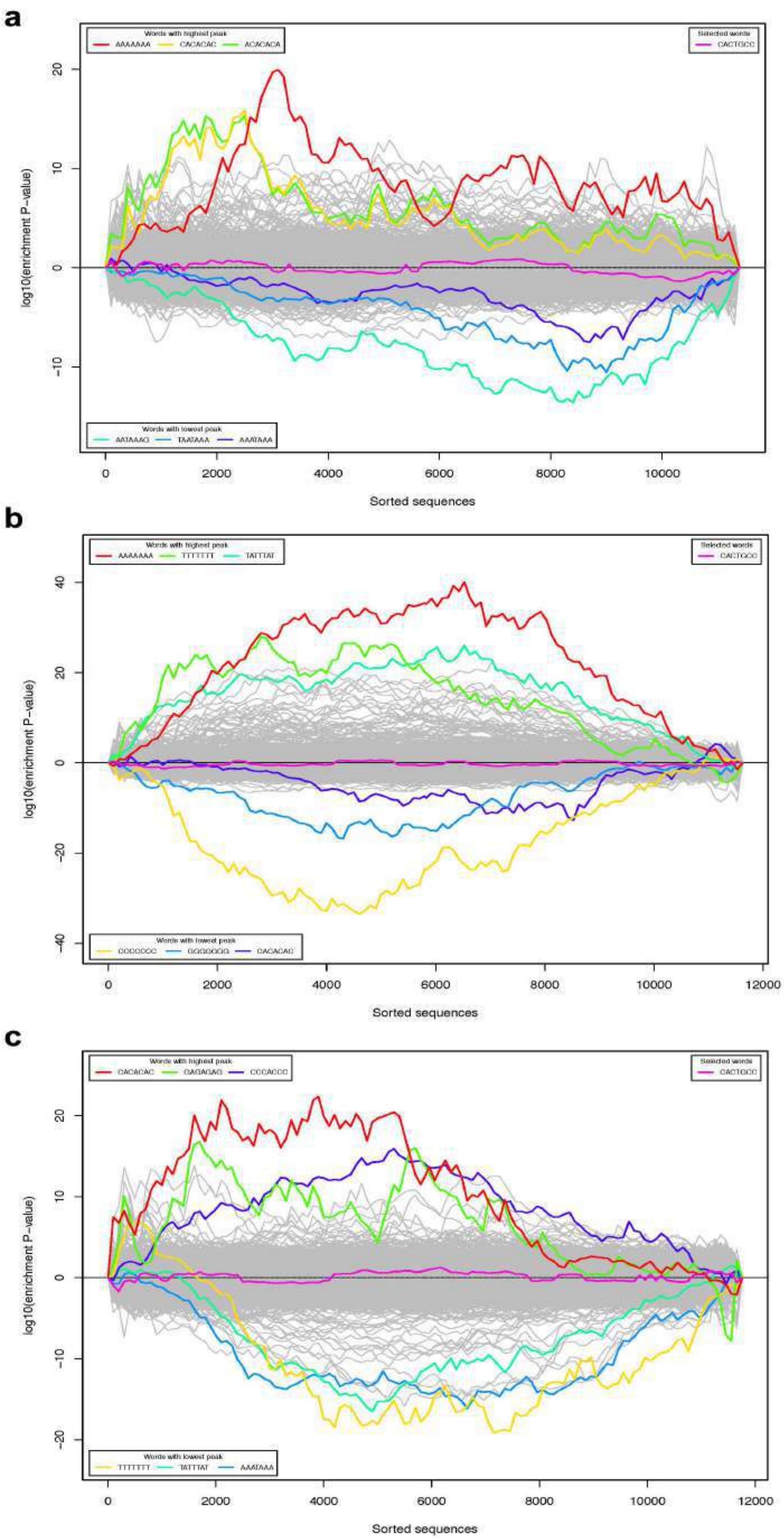

Figure S7. Sylamer analyses of the dysregulated mRNAs in male brains (a), female brains (b) and testes (c) of dKO mice at postnatal day 10 using the 7mer seed sequence, “GGCAGUG”, of the five miRNAs (miR-34b, miR-34c, miR-449a, miR-449b and miR-449c). The results suggest that the changes in mRNA transcriptome are likely caused by secondary effects due to dysregulation of miRNA direct targets in dKO organs.

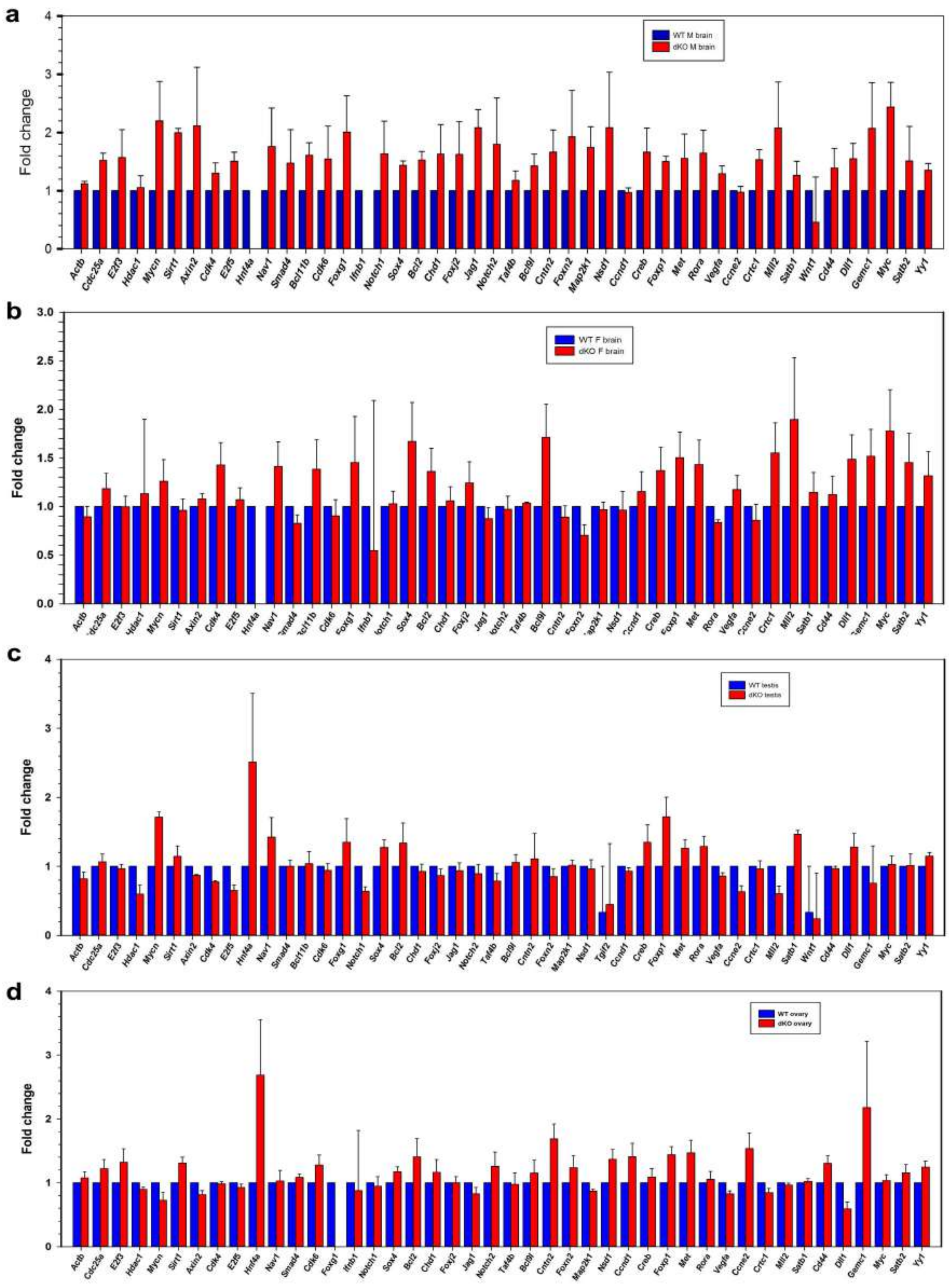

Figure S8. High throughput qPCR analyses of mRNA levels of 44 genes in WT and dKO male brain (**a**), female brain (**b**), testis (**c**), and ovary (**d**) at P10. The 44 genes examined are either validated or predicted targets for the five miRNAs of the miR-34b/c and miR-449 clusters. All qPCR assays were performed in biological triplicates. A total of 42, 39 and 40 out of 44 genes examined displayed similar changes between qPCR and RAN-Seq analyses in male brain, female brain and testis samples, respectively.

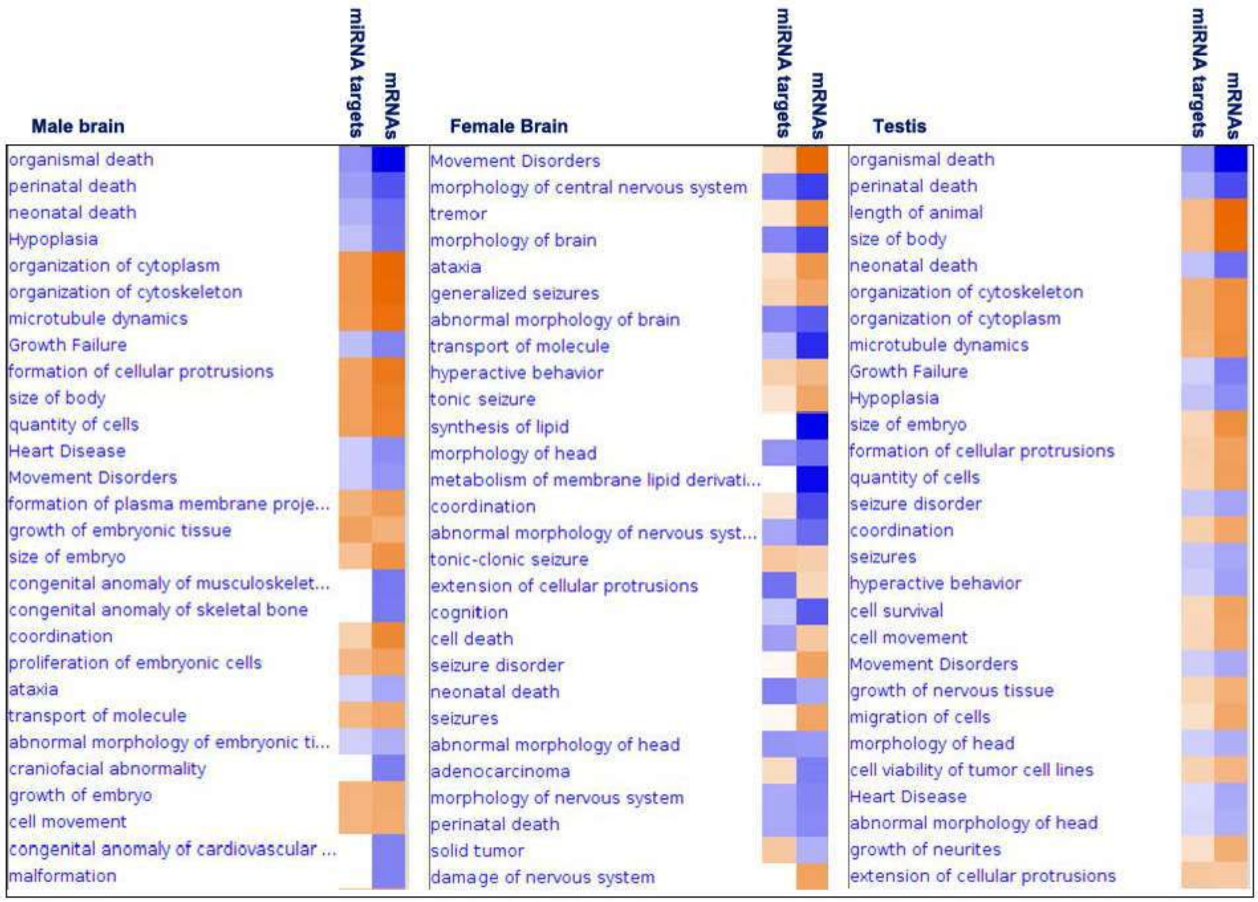

Figure S9. Gene ontology (GO) term enrichment analyses on dysregulated mRNAs and the targets of the five miRNAs in dKO brains (both male and female) and testes. RNA-Seq data were first processed using Tophat and Cufflinks followed by GO term enrichment analyses using Ingenuity (Qiagen).

Table S1. Body weight of dKO and control mice during postnatal development*.

	P3	P4	P5	P6	P7	P8	P9	P10	P11	P12	P13	P14	P15	P16	P17	P18	P19	P20
dKO female	1.88±0.23	2.41±0.32	2.68±0.4	3.05±0.45	3.56±0.57	4.03±0.68	4.48±0.69	4.77±0.7	5.15±0.79	5.56±0.8	6.01±0.8	6.3±0.78	6.47±0.81	6.53±0.95	6.51±1.04	6.65±1.14	6.74±1.29	7.03±1.37
con. female	2.27±0.31	2.75±0.47	3.28±0.43	3.78±0.42	4.4±0.43	5.08±0.5	5.6±0.59	6.12±0.66	6.66±0.77	7.25±0.92	7.64±1.05	8.05±1.2	8.35±1.28	8.53±1.26	8.36±1.17	8.31±1.16	8.73±1.16	9.23±1.15
P(dKO F vs.Con.F)	0.001911756	0.04246356	0.00067911	8.33676E-05	6.44979E-05	2.4984E-05	4.51293E-05	8.1991E-06	1.25729E-05	1.5738E-05	9.39724E-05	0.000151049	0.000118767	6.94327E-05	0.000120961	0.000547574	0.000124927	3.9266E-05
dKO male	1.73±0.22	2.27±0.38	2.58±0.44	2.99±0.57	3.31±0.65	3.6±0.6	3.83±0.67	4.03±0.72	4.29±0.64	4.62±0.77	4.76±1.06	5.13±1.1	5.45±1.08	5.66±1	6.01±0.73	6.21±0.45	6.19±0.65	6.24±0.84
con. male	2.64±0.49	3.15±0.56	3.76±0.51	4.24±0.5	4.84±0.53	5.54±0.71	6.03±0.74	6.52±0.82	6.98±0.91	7.44±0.98	7.9±1.16	8.21±1.26	8.53±1.4	8.76±1.36	8.89±1.36	9.15±1.38	9.68±1.43	10.23±1.31
P(dKO M vs.Con.M)	8.44955E-06	5.83129E-05	5.77818E-07	1.12049E-06	1.60863E-07	2.70212E-08	7.71361E-09	2.6435E-08	4.14826E-08	9.80434E-08	5.63503E-07	4.72953E-06	1.37834E-05	9.68681E-06	1.35316E-05	7.52738E-06	1.41002E-06	4.9629E-07

*Data are presented as mean ± SD and the P values were caculated usingthe student's *t*-test.

Table S2. Total number of significantly dysregulated mRNAs and the mRNAs targeted by the five miRNAs in dKO brains (male and female) and testes, as revealed by RNA-Seq analyses.

	GO-enriched cellular function						Total non-redundant	
	Cell fate control: Cancer genes, cell proliferation and apoptosis		Cytoskeleton organization: Microtubule dynamics and microfilament organization		Brain development: Abnormal development of head/brain			
No. dysregulated mRNA*	No. mRNAs	No. miRNA targets	No. mRNAs	No. miRNA targets	No. mRNAs	No. miRNA targets	No. mRNAs	No. miRNA targets
Male brain	1,559	66	440	28	398	28	2,863	86
Female brain	2,662	109	1,034	48	673	32	3,427	96
Testis	3,455	132	1,374	62	945	58	4,123	103
Total non-redundant	5,730	207	2,183	93	1,482	72	7,141	239

*Significance is defined by p<0.1

Yellow:

"organization of cytoskeleton" "organization of cytoplasm" "microtubule dynamics"
"morphology of cells" "formation of cellular protrusions" "cell movement"
"migration of cells" "development of body axis" "formation of plasma membrane projections"
"abnormal morphology of cells"

Green

"morphology of nervous system" "abnormal morphology of nervous system" "disorder of basal ganglia"
"morphology of head" "abnormal morphology of head" "morphology of central nervous system"
"abnormal morphology of brain" "morphology of brain" "neuritogenesis"
"development of central nervous system" "development of head" "development of brain"
"morphology of nervous tissue" "neurological signs" "neuromuscular disease"
"learning"

Red

"Cancer" "proliferation of cells" "epithelial neoplasia" "necrosis"
"carcinoma" "solid tumor" "cell death" "breast or colorectal cancer"
"apoptosis" "adenocarcinoma"

Table S3. Number of up- or down-regulated mRNAs and TargetScan-predicted miRNA targets and the percentage of upregulated mRNAs among all dysregulated mRNAs in dKO brains and testes.

		Upregulation*	Downregulation*	Unchanged	Total expressed gene (FPKM>=1)	Percentage of increased mRNAs (%)
Male brain	Dysregulated mRNAs	1,101	1,177	11,440	13,718	48%
	Dysregulated miRNA targets	64	9	318	391	88%
Female brain	Dysregulated mRNA	1,560	1,419	10,682	13,661	52%
	Dysregulated miRNA targets	48	46	300	394	51%
Testis	Dysregulated mRNAs	2,098	1,417	11,564	15,079	60%
	Dysregulated miRNA targets	85	17	300	402	83%

*Significance is defined by p<0.1; Expressed gene cutoff FPKM>=1.

Table S4. Target genes for miR-34b/c and miR-449a/b/c and their relative levels (dKO/WT ratio>1.0, upregulated; ratio<1.0, downregulated).

	miRNA targte genes	Mame brain_ratio_dKO/WT	Female brain_ratio_dKO/WT	Testis_ratio_dKO/WT
1	*2510009E07Rik*	1.074493524	1.165112783	1.417424463
2	*2610507B11Rik*	1.069147032	0.948487603	1.023010934
3	*3830406C13Rik*	0.720548603	0.990971382	0.805888857
4	*5730455P16Rik*	1.02930798	0.919744363	1.180659399
5	*9930012K11Rik*	0.818207884	1.249904866	0.718042623
6	*Abr*	1.071889163	0.979703004	1.457101146
7	*Acbd3*	1.136393879	0.994798257	1.236615707
8	*Acsl1*	1.16337451	0.841850976	1.234413037
9	*Acsl4*	1.087710929	0.77803964	1.169453321
10	*Actr1a*	1.073988979	1.11346567	0.943253169
11	*Adam22*	1.134419568	0.774083486	1.668309299
12	*Add2*	1.119847637	1.098187926	1.920966798
13	*Adipor2*	1.021705397	0.900066994	1.105591209
14	*Aff4*	1.206070241	0.944207608	1.148736565
15	*Agap2*	1.053809939	1.313302772	3.518384794
16	*Ahcyl2*	1.037252481	0.898078712	1.049141931
17	*Ahsa2*	1.043168212	1.051215796	1.223933431
18	*AI597479*	0.899773868	0.953736266	1.079228205
19	*Akap6*	1.150608301	1.064738103	7.759453138
20	*Alcam*	1.099536346	0.894205778	0.989840488
21	*Aldoa*	0.910384066	0.852087684	1.145975448
22	*Amer1*	1.304109614	1.190450811	0.990091795
23	*Ank3*	1.336041216	1.26941609	1.325110071
24	*Ankrd52*	1.137619433	1.134004542	0.99576424
25	*Anp32a*	0.951768546	0.92162894	1.466187745
26	*Arhgap1*	1.010727365	1.223602145	1.044362418
27	*Arhgap26*	1.203813628	0.993819759	1.073176024
28	*Arhgap36*	1.578009192	0.825140533	1.301554769
29	*Arid4a*	1.12624676	0.845030971	0.869919371
30	*Arid4b*	1.082915205	0.904990753	1.009872593
31	*Arl15*	0.927931151	1.086975167	1.280597504
32	*Asb1*	1.098727057	1.082100611	0.685618282
33	*Ascl1*	1.090334473	1.24709996	0.902383402
34	*Asic2*	1.092888161	1.051489595	6.016806153
35	*Atg4b*	0.95662887	0.963620326	0.86974614
36	*Atg9a*	1.100947369	0.90888606	0.999124328
37	*Atmin*	1.157027914	1.034360049	1.19401454
38	*Atoh1*	1.343175728	1.330793282	1.79150748
39	*Atxn7*	0.990964572	1.055638095	1.070111033
40	*Atxn7l3*	1.013911618	1.224355385	1.265707764
41	*AW549877*	0.895483212	0.905803941	1.161026527
42	*Axl*	1.036206602	1.18269427	1.150355696
43	*Baz2a*	1.094403102	1.149963381	0.9303602
44	*Bcl11b*	1.337018242	1.209047111	3.504555127
45	*Bcl2*	1.090071634	0.953847354	1.9848743
46	*Bnc2*	1.26235771	0.886764974	2.143745655
47	*Brpf3*	1.094703553	1.189805337	0.866927642
48	*Btbd11*	1.208693771	1.054447442	1.353385358
49	*C1ql3*	0.880484306	0.85266396	4.987241523
50	*Cacna1e*	1.34076284	1.112832845	5.614685088
51	*Cacna2d2*	1.492996909	1.047599132	1.321588231
52	*Cacnb3*	0.936500836	1.285683691	0.911885436
53	*Cacng2*	1.065708526	0.734311859	15.26249034
54	*Camsap1*	1.290848311	1.231365736	1.143568364
55	*Camta1*	NA	1.046056813	NA
56	*Cant1*	0.932721932	1.04081076	0.834478719
57	*Car7*	0.878481296	0.774462211	0.274623078
58	*Casp2*	0.997592174	1.123674557	1.224250332
59	*Cbfa2t3*	1.101354235	1.185147303	1.826981785
60	*Ccnd1*	0.93485076	1.125399545	1.110110857
61	*Ccne2*	NA	0.942458739	NA
62	*Cdc25a*	1.171351422	1.01181139	1.096744145
63	*Cdh4*	1.317368963	1.257571965	2.928316692
64	*Celf3*	1.005049538	1.216121757	3.722327575
65	*Chd1*	1.269034263	1.152096329	1.115406671
66	*Chl1*	1.400364137	1.258628788	6.873811861
67	*Clcn3*	1.113540326	0.796136332	1.275079328
68	*Clock*	0.955726318	0.706315206	1.008202582
69	*Cntn2*	1.376642432	0.988996046	8.025261983
70	*Cntnap1*	1.127569568	0.679869746	1.656364574
71	*Cntnap2*	1.078334705	1.063891721	7.782875177
72	*Col12a1*	1.004104945	1.421753721	1.502793124
73	*Cops7b*	0.867042576	1.106856997	0.946949742
74	*Coq2*	0.860004082	1.053468436	0.679316949
75	*Coro1c*	1.255383913	1.222750151	1.300541961
76	*Cpeb2*	1.109395784	1.071041054	0.873617809
77	*Cplx2*	0.996145988	1.07899993	3.867583374
78	*Crebrf*	1.048256355	0.737411999	1.023933519
79	*Crhr1*	0.917197172	1.098834543	1.192189974
80	*Crkl*	1.159330092	0.996158637	1.367208664
81	*Crtc1*	1.20770442	1.263050847	1.087306774
82	*Csf1r*	1.120810046	0.968246148	0.775427999
83	*Csnk1g1*	1.243761868	1.103509173	1.218800837
84	*Ctdsp2*	1.698035693	3.444576805	1.292908345
85	*Ctnnd1*	1.226572594	1.059143517	1.255546729
86	*Ctnnd2*	1.173517655	1.303686905	1.143481997
87	*Cuedc1*	1.124249285	1.192451577	0.966886246
88	*Cybrd1*	1.235419182	1.261649026	1.0984551
89	*Cycs*	0.705146368	0.877571881	0.812911958
90	*Daam1*	1.162954816	1.22922359	1.128051351
91	*Dcaf7*	1.19758762	1.059225018	1.256495193
92	*Dcp1a*	1.09722882	0.943320189	1.032016933
93	*Dcx*	1.375571695	1.504478012	2.5645199
94	*Ddn*	0.861553521	1.182408222	49.18595081
95	*Ddx17*	0.937026648	1.114038764	0.796910643
96	*Dgkz*	1.063367193	1.101037265	1.258760571
97	*Dixdc1*	1.170681927	0.945748182	1.307325067
98	*Dmwd*	NA	1.187808786	NA

99	*Dpysl4*	1.201817084	1.131618748	0.968895938
100	*E2f3*	1.025254051	0.937552983	1.220898922
101	*E2f5*	0.880871362	0.943517424	0.912687751
102	*Eea1*	1.242088285	0.923211727	1.114644197
103	*Elf4*	1.390982604	1.210529978	1.339194843
104	*Elmod1*	0.970009268	0.868716698	35.92160016
105	*Elmsan1*	1.179104048	NA	1.714677894
106	*Elovl6*	1.186603011	0.730122924	1.518340463
107	*Eml5*	0.857896659	1.093947042	0.672896791
108	*Eng*	1.406383858	0.703226671	1.080495992
109	*Epn2*	0.98188596	0.949251826	1.121242108
110	*Erc1*	1.309512593	1.111549347	1.339964854
111	*Ergic1*	1.050872069	1.086097517	1.043535171
112	*Esrra*	0.900071045	0.841369099	0.823829794
113	*Etl4*	1.076088446	0.86160477	1.116286784
114	*F2rl2*	1.867359766	0.832905569	0.686634901
115	*Faim2*	0.956588722	0.858187479	5.079477706
116	*Fam107a*	0.913544327	0.358248599	2.596478569
117	*Fam126b*	0.978759222	0.652075843	1.205353676
118	*Fam167a*	1.34010318	1.201603395	1.148931326
119	*Fam46a*	1.052504135	0.826763119	1.138341047
120	*Fam63b*	1.047109249	0.794981256	1.227017812
121	*Fam76a*	0.95461136	0.874040519	1.116053539
122	*Fam83h*	0.949369333	1.05255252	0.95513056
123	*Fat3*	1.396496553	1.262038116	2.880968038
124	*Fbln5*	1.022824646	0.524232982	1.029499153
125	*Fbxo10*	1.12955825	0.939517341	1.288104975
126	*Fbxo30*	1.14126639	0.798337373	1.411299091
127	*Fbxo41*	1.071865946	1.246652813	1.896649405
128	*Fgd6*	1.031923963	1.05517406	0.873389972
129	*Fgfr1*	1.276484556	0.935000337	1.139695116
130	*Fndc3b*	1.229674426	1.145141505	1.439631178
131	*Fndc8*	0.682102983	1.881284498	1.637886374
132	*Foxg1*	1.096945748	1.416265534	10.08119218
133	*Foxj2*	1.233299091	1.30846849	1.075436292
134	*Foxn2*	1.143685671	0.834082714	1.159047497
135	*Foxp1*	1.325102063	NA	2.040791139
136	*Foxp2*	1.099545283	1.190828919	2.855274752
137	*Frmd4a*	1.296904798	1.097576761	1.828883009
138	*Fut8*	0.995517069	0.905185589	0.984225365
139	*Fut9*	1.149501756	0.891595465	22.54055066
140	*Gabra3*	0.979000462	0.86303683	3.430561494
141	*Galnt7*	1.134744429	0.912749923	1.108566756
142	*Gas1*	1.116413945	1.051085949	1.073325155
143	*Gdap1l1*	0.986810601	1.122104674	2.642800167
144	*Glce*	25.56007635	17.4480222	2.086740787
145	*Gm973*	1.44773852	0.976270215	1.417169187
146	*Gmfb*	0.855245138	0.940280392	1.264189257
147	*Gmnc*	1.719840112	2.122924364	2.230713254
148	*Gnai2*	0.970298254	1.198134693	1.022438554
149	*Gnao1*	1.013550986	1.173195559	2.309516607
150	*Golph3l*	0.934999568	0.901305322	1.523393542
151	*Gpr101*	1.253922501	0.632262231	2.843305869
152	*Gpr158*	1.033253118	0.587143596	55.00004931
153	*Gpr22*	0.899089795	0.740009551	6.925260894
154	*Gpr64*	1.154508728	1.620440017	0.875743462
155	*Gpr85*	1.013163332	0.932301196	3.877551343
156	*Grem2*	0.929366902	0.897090041	2.107158138
157	*Grhl2*	1.202717286	2.393008047	0.984959919
158	*Grin2b*	1.587063102	1.36586312	24.13333254
159	*Grm7*	1.069245339	1.02989929	2.962087705
160	*Hcn3*	1.085391552	1.399327661	0.540731501
161	*Hecw2*	1.09171971	1.025206097	1.526283735
162	*Hk1*	1.244144765	1.129850399	1.636966788
163	*Hnf4a*	1.228266097	1.244597746	3.001646434
164	*Hook3*	1.285635278	0.880995478	1.144370881
165	*Htr2c*	1.077752233	0.689586056	12.71213387
166	*Igfbp3*	1.119849516	0.913040884	1.349570306
167	*Ing5*	1.003676995	0.909844207	1.039395432
168	*Inhbb*	1.048058439	1.043194984	1.489498495
169	*Inpp5a*	1.114485217	0.871745085	1.167057027
170	*Inpp5k*	1.013914793	0.98688347	0.947186307
171	*Irf2bp1*	1.200841044	1.05137245	1.248829642
172	*Itch*	1.022346912	0.824641149	1.042753399
173	*Itga10*	0.871667362	NA	0.778410116
174	*Itk*	1.166517429	1.421104016	0.96345164
175	*Itpripl1*	1.25027422	1.315499859	1.225044933
176	*Itsn1*	1.22779769	1.029160783	0.952447041
177	*Jag1*	1.538208173	0.924054862	1.076716711
178	*Jakmip1*	1.089836436	1.031042438	1.075460867
179	*Jmjd1c*	1.098785737	0.976129319	1.364806659
180	*Kalrn*	1.016321017	0.792385501	1.854120224
181	*Kcnd3*	1.291870844	0.989008381	0.787093914
182	*Kcne1l*	0.850556084	1.011730491	1.476387653
183	*Kcnk3*	1.005076487	0.89338731	0.622605918
184	*Kitl*	1.095668089	0.928132431	2.244669702
185	*Klhdc8a*	0.919067368	1.12698527	1.053336823
186	*Ldha*	0.871256694	1.10071079	1.342648779
187	*Lef1*	1.111577981	1.197548721	1.65332912
188	*Letmd1*	0.904589441	1.105021294	0.877081035
189	*Lgi1*	0.988516418	0.774548806	13.76535436
190	*Lgr4*	1.152823167	0.810499093	1.457779364
191	*Lhfpl4*	1.181220438	1.093628223	8.078958252
192	*Lima1*	1.198586244	0.677171539	1.07854685
193	*Limd2*	0.902908617	1.092572987	1.006667731
194	*Lman1*	0.983906341	0.79861218	1.169488439
195	*Lman2l*	0.850015709	0.950182325	0.571787966
196	*Lonrf3*	1.083582894	0.896538924	0.884933224
197	*Map1a*	1.272232373	1.175001509	1.952569518
198	*Map2k1*	0.859215264	0.839037594	1.420378279

199	*March5*	1.071975469	1.069845062	1.002694471
200	*Mcfd2*	0.769095286	0.796063545	0.793664835
201	*Met*	1.067518089	1.093545645	1.144541726
202	*Metap1*	1.032565379	1.055631566	1.055305332
203	*Mex3c*	1.01191897	0.890420657	1.55142494
204	*Mgat4a*	1.056654056	0.933145682	1.430761372
205	*Mgat5b*	1.166783724	1.249534171	0.491530529
206	*Mllt3*	0.93410248	0.972250334	1.281374259
207	*Mmab*	0.841581275	1.087581785	0.884176492
208	*Mpp2*	1.095080832	0.971747146	2.621877417
209	*Mpped2*	0.9543798	1.142625319	1.341125081
210	*Mras*	0.98190416	1.046937801	1.429869514
211	*Msl2*	1.073096129	1.121689418	1.310979234
212	*Mtus1*	1.194459544	0.803901036	1.421103953
213	*Mycn*	1.241414884	1.28762878	1.917855587
214	*Myh9*	1.369426887	0.987167058	1.519270961
215	*Myo1c*	1.14743404	1.181103352	1.195826679
216	*Myrip*	0.970725669	1.045271494	2.048891573
217	*N28178*	1.015850222	1.08694263	1.625026278
218	*Naa50*	1.025854879	0.964413043	1.392754218
219	*Nampt*	0.845800237	0.713111377	1.134242906
220	*Nav1*	1.234481696	1.682280729	1.499182286
221	*Nav3*	1.138560764	1.086488619	1.94003399
222	*Nceh1*	0.979524781	0.742629021	1.845811114
223	*Ndrg4*	0.969170048	0.832278648	2.358282289
224	*Ndst1*	1.208793579	1.105768783	1.172423365
225	*Neto1*	1.089756498	1.002068613	23.88315229
226	*Neurod2*	1.107521794	1.129646338	5.930095917
227	*Nfe2l1*	1.138171656	0.90265698	1.13249701
228	*Notch1*	1.320259909	1.168565293	0.776139607
229	*Notch2*	1.324907277	1.030735713	1.405244367
230	*Nptx1*	1.114840571	0.727137036	3.644461877
231	*Nrip3*	0.828757298	0.815712462	0.645448926
232	*Nrn1*	0.7787971	0.738261089	1.527039936
233	*Nrxn2*	1.247601277	1.250868028	1.947838824
234	*Nsd1*	1.368278827	0.997714379	1.033640594
235	*Nsmce4a*	0.926884456	1.027599584	0.976761391
236	*Nsun6*	1.074697745	1.13858295	0.875382706
237	*Ntn1*	1.354674648	0.913106387	1.122485647
238	*Numbl*	1.067187611	1.09686498	1.120369693
239	*Onecut2*	1.184668112	0.999001949	2.10087095
240	*Ormdl3*	0.958123788	1.000162245	0.895646621
241	*Osgin2*	0.942447283	0.874863579	0.927847086
242	*Oxsr1*	1.121202774	0.982406555	1.205155424
243	*Pacs1*	1.263406073	1.271584996	1.081448147
244	*Pclo*	1.179341411	1.527476672	1.110354079
245	*Pdgfra*	1.340767584	0.920624757	1.173225669
246	*Pdlim7*	0.848184748	1.149524353	1.147196712
247	*Pea15a*	0.888392339	1.171590035	0.982467943
248	*Peg10*	1.2238163	1.206136315	1.112732378
249	*Pgm2*	1.176807271	0.940679405	1.432497896
250	*Pgrmc2*	1.042206289	0.938525146	1.309058283
251	*Phf19*	0.905738451	1.617662992	0.902578766
252	*Pitpnc1*	1.125710496	1.068510648	1.141862795
253	*Pkia*	0.95353792	1.129383305	1.720817806
254	*Pkp4*	1.001334545	1.025981285	1.344527355
255	*Plekhg3*	1.254930664	0.576057057	1.014450435
256	*Plod1*	1.034144625	0.823059803	1.033353083
257	*Pnoc*	0.950486969	0.936406969	0.898772925
258	*Pogz*	1.153125775	1.218658385	1.254413926
259	*Pou3f3*	1.250659085	1.069351717	6.522528408
260	*Ppargc1b*	1.232766071	1.031112571	1.562368421
261	*Ppfia1*	1.045204613	1.003825011	1.229679101
262	*Ppp1r10*	1.134473413	1.063515587	0.968337886
263	*Ppp1r11*	0.821654222	1.12844156	0.680833485
264	*Ppp1r16b*	1.13616299	0.775315515	1.683286808
265	*Ppp1r1c*	1.823379443	0.925832348	0.557638321
266	*Ppp2r3a*	1.26831359	0.977006683	1.117350396
267	*Ppp4r2*	1.010258444	0.840391086	1.541406951
268	*Prex2*	1.155898318	0.958259416	1.50150568
269	*Prkacb*	0.98776974	0.966766844	1.53359661
270	*Prkd1*	1.170611823	0.987152417	1.065316738
271	*Prrg3*	0.997367233	1.016393335	1.231393226
272	*Psd3*	1.01243004	0.917087898	1.806285323
273	*Ptges*	0.890732731	1.072605568	1.911588523
274	*Ptpn4*	1.021387765	0.898443622	1.184425408
275	*Ptprm*	1.228173223	1.000806031	1.101738032
276	*Pvrl1*	1.681189574	1.207919176	1.864022572
277	*Rab43*	NA	1.130551671	NA
278	*Rai14*	0.936754253	0.778123058	1.135706876
279	*Ralgds*	1.127512462	1.072024394	1.409983437
280	*Ralgps2*	1.206400104	1.048178452	1.137595621
281	*Rap1gds1*	0.93991348	0.85608829	1.257327047
282	*Rdh11*	1.101092942	0.876363171	1.03864928
283	*Ret*	1.525542854	0.852825977	2.349993069
284	*Rfx3*	1.092598131	0.943007252	1.08810538
285	*Ric8b*	1.019967455	0.922636358	1.131971845
286	*Rnf152*	1.186857605	1.067928212	1.522518941
287	*Rnf165*	1.012299602	1.061340359	1.591609485
288	*Rnf34*	0.932715593	0.917546347	1.047528739
289	*Rnf41*	1.016572357	1.007529338	1.035039616
290	*Rnf44*	1.012402317	1.200169731	1.106888103
291	*Rps6ka4*	0.963033169	1.132675869	1.04181893
292	*Rps6kl1*	0.984702176	1.052595488	3.068687137
293	*Rragd*	0.944732043	1.046370535	1.50344483
294	*Rras*	1.159335288	0.879660209	1.349621807
295	*Rtf1*	1.060566644	1.040794221	1.228571889
296	*Rtn4rl1*	1.154954811	0.938939581	0.969102444
297	*Rufy2*	0.859010994	1.038864358	0.983192683
298	*Sash1*	1.053088868	1.091944702	1.245604558

299	*Satb1*	1.076040696	1.211271193	1.70074527
300	*Satb2*	1.383738717	1.578309502	2.077772605
301	*Scml2*	0.970263698	1.331951557	1.05143172
302	*Scn1a*	1.275976037	0.611521766	16.69452464
303	*Scn2b*	0.874117976	0.705852918	3.964333367
304	*Sec16a*	NA	1.080846437	NA
305	*Sec61a1*	1.092261913	0.909635021	0.920699822
306	*Sema4b*	1.242148085	1.202732137	0.970383901
307	*Sema4c*	1.334883399	1.201139492	1.223016455
308	*Sema4f*	1.097060987	1.102698129	0.779569856
309	*Sept3*	1.067530053	1.168964568	3.28405436
310	*Sept6*	0.930602314	1.051139259	0.708024424
311	*Serpine1*	1.205512271	0.478685993	1.069960662
312	*Serpinf2*	0.747188673	1.452343471	0.813354863
313	*Sfmbt2*	0.840854649	0.996756338	1.178709389
314	*Sgpp1*	0.995365244	0.823980628	1.16777655
315	*Sgsm2*	1.133788977	1.323170385	0.979692441
316	*Shank3*	NA	1.263034623	NA
317	*Shkbp1*	NA	1.171195074	NA
318	*Sidt1*	0.995159788	0.814655351	4.013428508
319	*Sidt2*	1.086590113	1.021341089	1.020919292
320	*Sipa1*	NA	0.951402477	NA
321	*Six3*	1.254041847	1.125592285	4.833058399
322	*Slc12a2*	1.357486461	0.740134792	1.368817013
323	*Slc16a2*	1.143156767	1.108072342	1.212759794
324	*Slc25a27*	0.927343429	1.015108645	0.760874223
325	*Slc27a4*	1.068228741	0.899088313	0.922101439
326	*Slc2a13*	1.138446405	0.820634289	2.634364691
327	*Slc2a3*	1.124948778	0.883943598	1.210758399
328	*Slc30a3*	0.843617954	0.914918859	1.743827711
329	*Slc35g2*	0.899378888	0.846520222	0.740287369
330	*Slc37a3*	0.980354429	0.90666299	1.069784965
331	*Slc44a2*	1.114429637	1.180635151	1.131140931
332	*Slc4a7*	1.165995296	1.00266318	0.906107787
333	*Slc6a1*	1.254559677	0.983320357	6.863675596
334	*Slc6a17*	1.149780492	0.86076421	3.906058022
335	*Slc7a2*	1.227563163	0.79111626	1.005034018
336	*Slc8a1*	1.365091523	1.057149363	1.698258763
337	*Slco3a1*	1.084342305	0.91139736	0.929171488
338	*Smc6*	1.157487796	0.901440229	1.414941027
339	*Smim15*	0.77652941	0.922838914	1.694306931
340	*Snap25*	0.876232102	0.745112461	56.62698086
341	*Snx12*	0.954160033	0.951760152	0.995642445
342	*Snx15*	0.956587508	1.030956929	1.134041985
343	*Snx30*	1.271504859	0.905223777	1.147118317
344	*Snx4*	0.94258622	0.932043465	1.243475504
345	*Sox12*	1.270450082	1.773608441	1.156515382
346	*Spcs2*	0.848814523	0.903741156	1.038481452
347	*Speg*	0.967282839	1.126158614	1.219896603
348	*Sprn*	0.912522939	0.897303462	1.452316718
349	*Spry3*	1	1	1
350	*Srpr*	0.88392637	0.802400871	1.056808031
351	*Stac2*	0.812041205	0.945108374	0.692980362
352	*Stat6*	0.89819295	1.082177377	0.954656665
353	*Stk38l*	0.959194945	0.907874561	1.035307414
354	*Strn3*	0.991967755	0.808289859	1.211239919
355	*Stx17*	0.89941442	1.081524284	0.89198839
356	*Suco*	1.137851589	0.951420893	1.025716774
357	*Svop*	0.974682628	0.979751239	9.923432779
358	*Syn2*	0.949446583	0.937050589	2.429611248
359	*Synj1*	1.087979909	1.038904322	0.797782396
360	*Syt1*	1.042624188	0.839879333	14.14070909
361	*Syvn1*	1.192970734	1.101535502	0.78660396
362	*Taf4b*	1.334249853	0.840613845	0.962372121
363	*Taf5*	0.916610318	0.944242877	1.178469889
364	*Tanc2*	1.247869367	1.317865995	0.8523676
365	*Tbck*	1.326502037	1.137081876	0.681022635
366	*Tbl1xr1*	1.174859743	0.946915627	1.276062758
367	*Tcam1*	1.20818814	1.084189096	0.809278116
368	*Tcf12*	1.102427237	0.826262391	1.249319213
369	*Tfdp2*	1.176240794	0.908425249	1.167672311
370	*Tfrc*	0.966002327	0.62592939	0.88449349
371	*Tgif2*	1.148727627	1.394211332	1.079864494
372	*Thumpd1*	1.015581711	0.925277207	1.257759779
373	*Tm9sf3*	1.022529678	0.817724985	1.352668042
374	*Tmcc3*	1.118170463	0.729206702	1.594888309
375	*Tmed8*	0.956967159	1.001012452	0.750168844
376	*Tmem109*	1.030926361	0.939971655	0.962973883
377	*Tmem134*	0.82560684	1.035939778	0.719684695
378	*Tmem150b*	0.970629507	1.241508079	1.139175985
379	*Tmem164*	1.114923584	1.11836471	1.265259296
380	*Tmem167b*	0.977149671	0.971104308	1.069470788
381	*Tmem184b*	1.094522088	0.876699167	1.211454685
382	*Tmem231*	1.158384678	NA	1.031694937
383	*Tmem246*	0.941204908	1.036530297	1.176893903
384	*Tmem255a*	1.088254318	0.769336604	0.416678164
385	*Tmem26*	1.352700343	1.425672632	1.438281516
386	*Tmem55a*	0.85128148	0.977226381	1.360069695
387	*Tnrc18*	1.261494485	1.428393058	1.382922618
388	*Tnrc6b*	0.056605398	1.056733857	0.1376985
389	*Tob2*	1.109368222	0.77055369	1.090603234
390	*Tpd52*	NA	0.879793144	NA
391	*Trank1*	0.837933161	1.845337426	0.799556084
392	*Trim67*	1.820019273	2.557517265	1.223110182
393	*Trim9*	1.055584959	1.036954087	1.991720783
394	*Trp53inp2*	0.862345118	0.894080061	0.965372135
395	*Ttc19*	0.871591739	0.854051902	1.124788949
396	*Tusc5*	0.837749863	1.112381306	0.851125024
397	*Txn1*	0.798430756	1.132657738	0.847177386
398	*Ube2g1*	0.905914923	0.884926748	1.184701288

399	*Ubn2*	NA	0.994153361	NA
400	*Ubp1*	0.946939188	1.180373997	0.799763189
401	*Ucn2*	1	2.066476362	1.493719568
402	*Uhrf2*	0.953478817	0.985442674	0.933984652
403	*Usp24*	1.218069286	1.112668112	1.103296609
404	*Usp31*	1.037759218	0.910540533	1.043128047
405	*Vamp2*	0.898517347	1.173299816	1.177573913
406	*Vat1*	1.309556826	1.242029485	1.2803351
407	*Vcl*	1.285515178	0.751582905	1.239286019
408	*Vwa5b2*	0.929012253	1.671606825	1.826022056
409	*Wasf1*	1.007323742	1.132258598	1.379495884
410	*Wdr37*	1.01170322	0.767279708	1.227980125
411	*Wnt1*	0.991113152	1.325631723	3.078599415
412	*Wscd2*	1.068808264	0.951543724	2.163419096
413	*Wtap*	0.918516338	0.96053148	1.100020527
414	*Yy1*	1.064657616	1.021942012	1.080538174
415	*Zc3h4*	1.272487334	1.193778506	0.98299752
416	*Zdhhc16*	0.972734968	1.020351263	0.895391431
417	*Zdhhc17*	1.106198502	0.769558719	1.28207868
418	*Zer1*	1.151129405	1.150818752	0.998637833
419	*Zfhx4*	1.215609824	1.326678527	1.401999908
420	*Zfp275*	1.018854018	0.940174131	1.27285636
421	*Zfp281*	1.084900809	0.900536092	1.435547811
422	*Zfp282*	1.127974849	NA	1.54227545
423	*Zfp316*	1.202906953	1.170935091	1.242182814
424	*Zfp553*	1.28285502	0.909085093	1.31726944
425	*Zfp593*	0.859923131	1.169046538	0.865669313
426	*Zfp641*	1.118470937	1.061152504	0.72701927
427	*Zfp644*	1.048067345	0.940437311	1.604816814
428	*Zmym4*	1.24341549	1.001610932	1.359989178
429	*Soga1*	NA	NA	NA
430	*Arhgap39*	NA	NA	NA
431	*B4galt2*	NA	NA	NA
432	*Brinp1*	NA	NA	NA
433	*Kmt2d*	NA	NA	NA
434	*Mta2*	NA	NA	NA
435	*Palm2*	NA	NA	NA
436	*Jade2*	NA	NA	NA
437	*Lzts3*	NA	NA	NA
438	*Synj2bp*	NA	NA	NA
439	*Usf1*	NA	NA	NA

Table S5. Primers used for genotyping and TaqMan-based miRNA qPCR analyses.

Name	Sequence (5'-3')	Usage
miR-449-For	GATTCTCACAACTGATGTAG	genotyping
mir-449-Rev1	ACAATGGTTAGTACTTTCAC	genotyping
miR-449-Rev2	ATGCACAGATATAAGTGCAG	genotyping
miR-34bc-KO-F2	GCGGCCGCATAACTTCGTAT	genotyping
miR-34bc-Com-L2	GAGATTTTCGTGGCGCTTTA	genotyping
miR-34bc-WT-U2	GCCTCCTGTGAATCGTCATT	genotyping
mmu-miR-449a-5p	TGGCAGTGTATTGTTAGCTGGT	miRNA qPCR
mmu-miR-449b	AGGCAGTGTTGTTAGCTGGC	miRNA qPCR
mmu-miR-449c-5p	AGGCAGTGCATTGCTAGCTGG	miRNA qPCR
mmu-miR-34b-5p	AGGCAGTGTAATTAGCTGATTGT	miRNA qPCR
mmu-miR-34c-5p	AGGCAGTGTAGTTAGCTGATTGC	miRNA qPCR
U6	GCAAATTCGTGAAGCGTTCC	miRNA qPCR
RTQ-UNIr	CGAATTCTAGAGCTCGAGGCAGG	miRNA qPCR
Probe	FAM-CTCGGATCCACTAGTC-MGB	miRNA qPCR
miRTQ primer	CGAATTCTAGAGCTCGAGGCAGGCGACATGGCTGGCTAGT TAAGCTTGGTACCGAGCTCGGATCCACTAGTCC(T25)VN	miRNA cDNA library

In RTQ primer, V is A, G, or C; N is A, G, C, or T.

Table S6. High-throughput real time PCR primer sequences.

Gene Symbol	Forward Primer	Reverse Primer	Gene Full Name
Actb	CCCTAAGGCCAACCGTGAAA	AGCCTGGATGGCTACGTACA	actin, beta
Axin2	GATCCACGGAAACAGCTGAA	AGCCGGAACCTACGTGATAA	axin2
Bcl11b	AGCACTTGTCCCAGAGGGAA	TCTCCAGACCCTCGTCTTCC	B cell leukemia/lymphoma 11B
Bcl2	ATGTGTGTGGAGAGCGTCAA	GATGCCGGTTCAGGTACTCA	B cell leukemia/lymphoma 2
Bcl9l	GGAAGCTGGGACTCCATCC	CAGCACACACCTCCGTTTAC	B cell CLL/lymphoma 9-like
Ccnd1	TGCCGAGAAGTTGTGCATCTA	TGTTCACCAGAAGCAGTTCCA	cyclin D1
Ccne2	GCTGCCGCCTTATGTCATTTA	CCGAGATGTCATCCCATTCCA	cyclin E2
Cd44	GTCACAGACCTACCCAATTCC	TACTCGCCCTTCTTGCTGTA	CD44 antigen
Cdc25a	TTGGACAGTGACCCAAGAGAC	AATCCTGATGCTTCCCAGAGAC	cell division cycle 25A
Cdk4	ATGTGGAGCGTTGGCTGTA	TGGTCGGCTTCAGAGTTTCC	cyclin-dependent kinase 4
Cdk6	TGGAAGTTCAGACGTGGATCA	GTCCCTAGGCCAGTCTTCC	cyclin-dependent kinase 6
Chd1	GGTTTAAACTGGCTCGCTCAC	TTCCCAAGGCCCATTTCATCA	chromodomain helicase DNA binding protein 1
Cntn2	GCTGATGCCATGACCATGAA	ACTTAAGGCTGAGGCTGGAA	contactin 2
Crebbp	GACAGCTGTTTACCATGAGATCC	GGCCCAAATATGTCCTGTCAC	CREB binding protein
Crtc1	TCTCCAACCAAGGCTTCTCC	CATAGTACGCATCCCCAAACAC	CREB regulated transcription coactivator 1
Dll1	TGGCTGGAAAGGCCAGTAC	CCCTGGTTTGTCACAGTATCCA	delta-like 1 (Drosophila)
E2f3	ATATCCCCAAGCCCACTTCC	CAGAGGAGAGAGGTTTGCTGTA	E2F transcription factor 3
E2f5	TGGGCTTGCTTACCACCAA	TTTGCCTCACAGCCAAGGTA	E2F transcription factor 5
Foxg1	GCCAGCAGCACTTTGAGTTA	TGAGTCAACACGGAGCTGTA	forkhead box G1
Foxj2	GTCCTTCCGCAACCTCTACAA	TGTCTCCCAGGAGTGAGGAAA	forkhead box J2
Foxn2	CACTGCTTAAGCTCTGCTCTCA	CATTGCAGTGGCTGCATCAA	forkhead box N2
Foxp1	CGGAGGCCACAAAAGATCA	GCATTGAGAGGTGTGCAGTA	forkhead box P1
Gapdh	AGACGGCCGCATCTTCTT	TTCACACCGACCTTCACCAT	glyceraldehyde-3-phosphate dehydrogenase
Gm606	ACAACACTGAGCTCCAGCAA	AACATGAGTCCAGAACAGGGAA	predicted gene 606
Hdac1	TGACATCGTCCTGGCCATC	GCCATCGCCATGGTGAATATC	histone deacetylase 1
Hnf4a	AGGAGGAGCGTGAGGAAGAA	TGCAGTAACGACACTGGTTCC	hepatic nuclear factor 4, alpha
Ifnb1	TACACTGCCTTTGCCATCCA	CCACCCAGTGCTGGAGAAA	interferon beta 1, fibroblast
Jag1	TCCCAAGCATGGGTCTTGTA	GATGCACTTGTCGCAGTACA	jagged 1
Map2k1	ACCTATCTTCGGGAGAAGCA	ATCTCCCCACGTGAGTTCA	mitogen-activated protein kinase kinase 1
Met	GGCTCTTCCTGTGGATGAGAA	GTACTCTTGCGTCATAGCGAAC	met proto-oncogene
Mll2	TCACCCGTACTGTGTCAACA	CACACACGATACACTCCACAC	lysine (K)-specific methyltransferase 2D
Myc	AGTGCTGCATGAGGAGACA	TCTCCACAGACACCACATCAA	myelocytomatosis oncogene
Mycn	GCACCTCCGGAGAGGATAC	GACGCACAGTGATCGTGAAA	v-myc myelocytomatosis viral related oncogene, neuroblastoma derived (avian)
Nav1	GGAGCGTTAAATGCCTCAGAA	TGTTGAGGCTGGAGATGCTA	neuron navigator 1
Notch1	GGACGGCGTGAATACCTACA	GACATTCGTCCACATCCTCTGTA	notch 1
Notch2	TGGTTCTGGGACAAGTGAACA	ACAGCAAAGCCTCATCCTCA	notch 2
Nsd1	TTATGCCCAAGAAGGGTGAC	GCCCGTGATTCAACAATACC	nuclear receptor-binding SET-domain protein 1
Rora	AGAACCACCGAGAAGATGGAA	GTCGTCCACATAGGGCTCTTA	RAR-related orphan receptor alpha
Satb1	TAAAACACTCGGCCATCTCA	TGTTCCACCACGCAGAAAAC	special AT-rich sequence binding protein 1
Satb2	CCAGGAGTTTGGGAGATGGTA	TGAAAGGTTCTCTCGCTCCA	special AT-rich sequence binding protein 2
Sirt1	CTGAAAGTGAGACCAGTAGCA	GATGAGGCAAAGGTTCCCTA	sirtuin 1
Smad4	CCAACATTCCTGTGGCTTCC	GCTATCTGCAACAGTCCTTCAC	SMAD family member 4
Sox4	CATGTCCCTGGGCAGTTTCA	CTGAGCCGGGTTCGAAGTTAA	SRY-box containing gene 4
Taf4b	CAGACAGCCAAAGTCAAGCA	GGAATGGGAAATGGAGGTCAC	TAF4B RNA polymerase II, TATA box binding protein (TBP)-associated factor
Tgif2	GTCAGACCCGGCAGGTAC	CGACATGATGCTTAGGGGCTA	TGFB-induced factor homeobox 2
Vegfa	CCAGCACATAGGAGAGATGAG	CTGGCTTTGTTCTGTCTTTCTT	vascular endothelial growth factor A
Wnt1	CGCTTCCTCATGAACCTTCAC	TGGCGCATCTCAGAGAACA	wingless-related MMTV integration site 1
Yy1	CAAGAACAATAGCTTGCCCTCA	GGTGTGCAGATGCTTTCTCA	YY1 transcription factor